Imprinted X-inactivation in extra-embryonic endoderm cell lines from mouse blastocysts

Tilo Kunath[1,2,*], Danielle Arnaud[3], Gary D. Uy[4], Ikuhiro Okamoto[5], Corinne Chureau[3], Yojiro Yamanaka[1], Edith Heard[5], Richard L. Gardner[4], Philip Avner[3,†] and Janet Rossant[1,2,†]

[1]Samuel Lunenfeld Research Institute, Mount Sinai Hospital, 600 University Avenue, Toronto M5G 1X5, Canada
[2]Department of Molecular and Medical Genetics, University of Toronto, Toronto M5S 1A8, Canada
[3]Unité de Génétique Moléculaire Murine, URA 2578 CNRS, Institut Pasteur, 25 rue du Docteur Roux, Paris 75015, France
[4]Mammalian Development Laboratory, Department of Zoology, University of Oxford, South Parks Road, Oxford, OX1 3PS, UK
[5]CNRS UMR218, Curie Institute, 26 rue d'Ulm, Paris 75005, France
*Present address: Institute for Stem Cell Research, University of Edinburgh, King's Buildings, West Mains Road, Edinburgh, EH9 3JQ, UK
†Authors for correspondence (e-mail: rossant@mshri.on.ca and pavner@pasteur.fr)

Accepted 27 January 2005

Development 132, 1649-1661
Published by The Company of Biologists 2005
doi:10.1242/dev.01715

Summary

The extra-embryonic endoderm lineage plays a major role in the nutritive support of the embryo and is required for several inductive events, such as anterior patterning and blood island formation. Blastocyst-derived embryonic stem (ES) and trophoblast stem (TS) cell lines provide good models with which to study the development of the epiblast and trophoblast lineages, respectively. We describe the derivation and characterization of cell lines that are representative of the third lineage of the blastocyst – extra-embryonic endoderm. Extra-embryonic endoderm (XEN) cell lines can be reproducibly derived from mouse blastocysts and passaged without any evidence of senescence. XEN cells express markers typical of extra-embryonic endoderm derivatives, but not those of the epiblast or trophoblast. Chimeras generated by injection of XEN cells into blastocysts showed exclusive contribution to extra-embryonic endoderm cell types. We used female XEN cells to investigate the mechanism of X chromosome inactivation in this lineage. We observed paternally imprinted X-inactivation, consistent with observations in vivo. Based on gene expression analysis, chimera studies and imprinted X-inactivation, XEN cell lines are representative of extra-embryonic endoderm and provide a new cell culture model of an early mammalian lineage.

Key words: Primitive endoderm, X-inactivation, Chimeras, Embryonic stem cells

Introduction

Trophectoderm and primitive endoderm (PrE) are the founding cell types for two major, but distinct, extra-embryonic lineages. During mouse blastocyst formation at embryonic day 3.5 (E3.5), trophectoderm forms the outer layer of the blastocyst and by E4.5, just prior to implantation, PrE forms on the blastocoel-exposed surface of the inner cell mass (ICM) (Fig. 1A). By E5.0, the PrE is segregating into two subpopulations of extra-embryonic endoderm: visceral endoderm (VE) and parietal endoderm (PE) (Enders et al., 1978). PE cells grow with minimal cell-cell contact as they scatter on the inner surface of the giant cell layer (Fig. 1A) (Hogan and Tilly, 1981). They secrete copious amounts of basement membrane proteins to form Reichert's membrane in conjunction with the trophoblast giant cell layer (Hogan et al., 1980). The combination of PE cells, giant cells and the intervening thick basement membrane comprises the early functioning, transient parietal yolk sac (Dickson, 1979). PrE in contact with the epiblast and extra-embryonic ectoderm (trophoblast) differentiates into an epithelial sheet of visceral endoderm (Fig. 1A). VE cells in contact with extra-embryonic ectoderm are more columnar and cuboidal, while VE cells covering the epiblast are flatter and more epithelial in shape (Solter et al., 1970). They also exhibit differences in gene expression. For example, α-fetoprotein is expressed in VE overlying the epiblast (Dziadek, 1978), while *Sox7* and *Cited1* are abundant in VE overlying extra-embryonic ectoderm (Dunwoodie et al., 1998; Kanai-Azuma et al., 2002). Distal VE cells at E5.5 move asymmetrically to the future anterior region of the embryo and become anterior VE (AVE) (Thomas et al., 1998; Srinivas et al., 2004). This subset of cells appears thicker during their anterior movement and they specifically express genes not present in other parts of the VE, such as *Hex*, *Cer1* and *Otx2* (Ang et al., 1994; Biben et al., 1998; Thomas et al., 1998). The AVE induces anterior character on the overlying ectoderm by repressing posterior fates (Thomas and Beddington, 1996; Yamamoto et al., 2004). By E8.0, extra-embryonic mesoderm has become closely associated with VE to form the visceral (definitive) yolk sac. In this tissue, the VE plays an inductive role, via Indian hedgehog and VEGF, in formation of blood islands and endothelial cells (Dyer et al., 2001; Byrd et al., 2002; Damert et al., 2002).

Permanent cell lines with properties of the epiblast (embryonic stem cells) and the trophoblast (trophoblast stem cells) have been established and characterized (Evans and Kaufman, 1981; Martin, 1981; Tanaka et al., 1998). However,

reproducible derivation of cell lines with properties of the primitive endoderm lineage, including the ability to repopulate the lineage in vivo, has not been reported. The F9 embryonal carcinoma cell line has proven to be a useful model for studying VE and PE differentiation in culture (e.g. Kanungo et al., 2000; Verheijen et al., 1999b). Several other cases of cell culture models of extra-embryonic endoderm have been described previously: parietal endoderm cell (PEC) lines derived from mouse blastocysts (Fowler et al., 1990); the yolk sac carcinoma line, L2, from the rat (Wewer, 1982); and the RE1 line derived from a rat blastocyst (Notarianni and Flechon, 2001). Molecular characterization of these lines has, however, not been extensively performed, and their ability to participate in normal development remains unknown.

Described here is the characterization of cell lines representative of the extra-embryonic endoderm lineage that can be reproducibly derived from mouse blastocysts. They express a molecular profile particular to this lineage and, importantly, they are developmentally restricted to form extra-embryonic endoderm in vivo. Our first use of this novel system was to investigate the status and mechanism of X-chromosome inactivation in female XEN cells. We show XEN cells exhibit paternally imprinted X-inactivation, and that they show a novel combination of epigenetic modifications on the imprinted X, suggesting that trophoblast and extra-embryonic endoderm lineages may differ in their imprinting maintenance mechanisms.

Materials and methods

XEN cell line derivation and culture conditions

Extra-embryonic endoderm (XEN) cell lines were derived by three methods. Four lines where derived from the PO strain (Oxford University, Oxford). E3.5 blastocysts, hemizygous for the ROSA26 βgeo transgene (Zambrowicz et al., 1997), were subjected to immunosurgery to isolate their inner cell masses (ICMs) (Hogan et al., 1994; Lin, 1969). ICM pairs were aggregated and incubated overnight to obtain mini blastocysts, which were plated on embryonic fibroblasts (EMFIs) in TS cell line derivation conditions (Uy et al., 2002). The resulting blastocyst outgrowths were disaggregated 2-3 days after attachment. Although TS cell colonies were present, the vast majority of the cells were XEN cells. The XEN cell lines were designated IM5A1, IM8A1, IM8A2 and IM9C4. In the second method, XEN cell lines were derived from wild-type ICR embryos. E3.5 blastocysts were plated in four-well plates on EMFIs in RPMI 1640 (Gibco) supplemented with 20% fetal bovine serum (FBS) (CanSera, Rexdale, Canada), 1 mM sodium pyruvate, 2 mM L-glutamine, 50 mg/ml each of penicillin/streptomycin (all from Gibco), 100 μM β-mercaptoethanol (Sigma), 25 ng/ml human recombinant FGF4 (hrFGF4) and 1 μg/ml heparin (both from Sigma). The medium was changed every 3 days and the blastocyst outgrowths were not disaggregated. After 15 days, XEN cells, observed in half the cultures, were passaged 1:1 onto new EMFIs in four-well plates. Three XEN cell lines, XEN1-2, XEN1-3 and XEN1-4, derived in this manner, were routinely cultured on EMFIs in medium without FGF4 and heparin or on gelatin (0.1% porcine skin gelatin, Sigma) supplemented with 70% EMFI-conditioned medium (EMFI-CM) (Tanaka et al., 1998). A third series of XEN lines were isolated from Tgn (X^{GFP}) 4 Nagy × 129Hprt^{bm1}Pgk1a blastocysts using standard LIF-containing GMEM medium (Gibco) without FGF4 (Morey et al., 2004). Three XEN cell lines were obtained by this method: GHP7/3. GHP7/7 and GHP7/9. Selection was performed in HAT medium (100 μM hypoxanthine, 0.4 μM aminopterin, 16 μM thymidine) and 6-thioguanine (10 μg/ml). Of the various culture conditions described, we found XEN cells were the most robust in 70% EMFI-CM on gelatin and most experiments were performed under these conditions. Cells were routinely fed every 2 days and passaged at 1:10 to 1:20 every 4 days. Each XEN cell line has been cryopreserved and recovered with high viability. XEN cells were differentiated by plating them directly onto cell culture plastic, in the absence of gelatin, and culturing for 4 or 8 days in supplemented RPMI 1640 medium (described above) without hrFGF4, heparin or EMFI-CM.

ES and TS cell cultures

HP3.10 female ES cell line have been described previously (Clerc and Avner, 1998). F3 trophoblast stem cell line was isolated from F1 129/Sv Hprt-4 Pgk1a × 129/Sv embryos using a published protocol (Tanaka et al., 1998) and maintained in RPMI 1640 (Gibco) with 20% FBS (Gibco), 1 mM sodium pyruvate, 2 mM L-glutamine, 50 mg/ml each of penicillin/streptomycin (all from Gibco), 100 μM β-mercaptoethanol (Sigma), 25 ng/ml hrFGF4 and 1 μg/ml heparin (both from Sigma).

DNA transduction of XEN cells

IM8A1 cells were co-electroporated with pCX-EGFP and pPGK-puro plasmids. IM8A1 cells (5×10^6 cells at passage 39) were resuspended in PBS (0.8 ml) and transferred to a GenePulser Cuvette (0.4 cm electrode, BioRad catalog number 165-2088). *Sca*I-linearized pCX-EGFP plasmid (18 μg) (Hadjantonakis et al., 1998) and *Eco*RI-linearized pPGK-Puro plasmid (2 μg) were added to the cell suspension and electroporated (0.25 V, 500 μF). The cells were incubated on ice (20 minutes) and plated in 70% EMFI-CM (10 ml) on a gelatinized 100 mm plate. Drug selection (puromycin, 1 μg/ml) was started 1 day later, and at 12 days the colonies were passaged and expanded as a pool before FACS-sorting for GFP-positive cells (see below).

FACS analysis and subclonal lines

GFP-IM8A1 cells at one passage after electroporation (see above) were FACS-sorted for GFP fluorescence with an argon ion laser (488 nm). Approximately 800,000 GFP-positive cells were sorted into 70% EMFI-CM + G418 (90 μg/ml) + Puro (1 μg/ml) medium and plated on 0.1% gelatin in a 60 mm dish. To derive subclonal lines, 192 GFP-positive cells were single-cell sorted directly into 96-well plates.

PCR sexing

XEN cells (per single well of a four-well plate) were lysed in 100 μl of 0.1 mg/ml Proteinase K (Boehringer Mannheim) in a solution of 50 mM KCl, 10 mM Tris.HCl (pH 8.3), 2 mM $MgCl_2$, 0.1 mg/ml gelatin (Sigma), 0.45% Nonidet P-40, and 0.45% Tween-20. PCR genotyping was performed for the X-chromosome-specific *Xist* gene and Y chromosome-specific *Zfy1* gene. The primers are Xist (5′-TTG-CGGGATTCGCCTTGATT-3′) and (5′-TGAGCAGCCCTTAAAGC-CAC-3′); Zfy1 (5′-GCATAGACATGTCTTAACATCTGTCC-3′) and (5′-CCTATTGCATGGACAGCAGCTTATG-3′). PCR was performed at an annealing temperature of 65°C in 1.5 mM $MgCl_2$ for 35 cycles. The first four cycles had a 4 minute melting time at 95°C, while the next 31 cycles had a 1 minute melting time. The predicted Xist PCR product is 207 bp and Zfy1 is 183 bp. The IM5A1, IM9C4, GHP7/3 and GHP7/9 lines were genotyped as female and the XEN1-3 and GHP7/7 lines were genotyped as male (Table 1).

Videomicroscopy

XEN cells (GFP-IM8A1, subclone 1) at passage 50 were cultured on a gelatinized 100 mm plate in 70% EMFI-CM (50 ml). The microscope chamber was maintained at 37°C and 5% CO_2. Phase-contrast images were taken every 2 minutes for 12 h at 200× magnification. The imaging application used was Simple PCI by Compix (Cranberry Township, PA). The behavior of 25 XEN cells was traced for 9 out of the 12 hours. False-color (red and blue) was added to two cells using Adobe Photoshop 6.0 in 51 frames (100

minutes) of footage and the final online movie was generated with iMovie 3.

Scanning electron microscopy

XEN cells (IM8A1 at passage 29) were plated on round, plastic Thermanox coverslips (Nunc, Mississauga, Canada) in four-well plates in 70% EMFI-CM and cultured for 2 days. The cells were washed with PBS and fixed in 2% glutaraldehyde in 0.1 M phosphate buffer at 4°C overnight. The specimens were then post-fixed in 1% osmium tetroxide in the same buffer, rinsed with 0.1 M phosphate buffer and dehydrated in a graded ethanol series. The coverslips were then critical-point dried in a Bal-Tec CPD 030, mounted on aluminum stubs and sputter coated with gold in a Denton Desk II. Imaging was carried out on an FEI XL30 ESEM under standard high vacuum conditions. Most images were taken at 0° (perpendicular to the mounting stage) and some were taken at a 60° angle.

RT-PCR analysis

Total RNA was isolated from XEN cells, ES cells and embryoid bodies using the Qiagen RNeasy midi kit (Qiagen, Santa Clarita, CA) according to manufacturer's instructions. cDNA was prepared by annealing a dT_{12-18} primer (1.0 μl of 0.5 μg/μl) to 460 ng (11 μl) of total RNA at 65°C for 5 minutes. 5× RT buffer (4 μl, Invitrogen), 0.1 M DTT (2 μl), 10 mM dNTPs (1 μl) and Superscript II reverse transcriptase (1 μl, Invitrogen) were added and incubated at 42°C for 1 hour. The resulting cDNA was analyzed for the following markers: *Afp*, *Gata4*, *Sox7*, *Hnf4*, *Foxa2*, *Oct4* and β-actin (see Table S1 in the supplementary material).

Affymetrix analysis

Three biological replicates of XEN cell RNA were submitted to the Centre for Applied Genomics at the Hospital for Sick Children (Toronto, Canada) for preparation of cRNA and hybridization to the mouse U74Av2 Affymetrix gene array (Liu et al., 2003). Qiagen RNeasy midi kit (Qiagen, Santa Clarita, CA) was used to extract total RNA from all samples according to manufacturer's instructions. The samples were: (1) XEN1-3 cells at passage 18 (ICR strain, male) cultured on gelatin with 70% EMFI-CM; (2) IM8A1 cells at passage 27 (PO strain) cultured on gelatin with 70% EMFI-CM; and (3) IM8A1 cells at passage 27 cultured on tissue culture plastic in RPMI 1640 (Gibco) supplemented with 20% FBS (CanSera, Rexdale, Canada), 1 mM sodium pyruvate, 2 mM L-glutamine, 50 mg/ml each of penicillin/streptomycin (all from Gibco), 100 μM β-mercaptoethanol (Sigma) for 4 days. RNA was also obtained from R1 ES cells grown in the absence of EMFIs in standard conditions (Nagy et al., 1993) and subjected to the above analysis. A threshold significance value of $P<0.04$ was used to consider a gene expressed or 'present' and $P>0.06$ for genes not expressed or 'absent' and marginal values were $0.04<P<0.06$. Ratio data were obtained using Affymetrix MAS 5.0 software. GEO Accession Number is GSE2204.

Production of XEN cell chimeras

GFP-IM8A1 cells from a GFP-sorted population (passage 43) and from a subclonal line (GFP-IM8A1-4, passage 46) were injected into E3.5 ICR blastocysts. Between 10 and 15 XEN cells were injected per embryo and transferred to the uterus of E2.5 pseudopregnant ICR females. Dissections were performed at E6.5, E7.5 and E8.5 with special attention taken to keep the parietal yolk sac intact. X-gal staining of embryos was performed as previously described (Rossant et al., 1991). Experimental animals were treated according to guidelines approved by the Canadian Council for Animal Care.

Allelic quantitative real-time RT-PCR

Quantitative real-time PCR measurements of *Xist* cDNA were carried out using TaqMan fluorescent probes and TaqMan Universal PCR Mix and an ABI Prism 7700 (Perkin Elmer Applied Biosystem) as previously described (Morey et al., 2001). *Xist* cDNA quantitations were internally standardized against the endogenous *18s* rDNA gene. Quantitative real-time PCR measurements of *Nap1l2* cDNA were performed using SYBR Green Universal Mix. Two informative SNPs identified between the 129 and Pgk alleles were used to design allele-specific primers: Nap1l2-129-F (5′-GCACCGTCTTTTATCCC-CACT-3′), which is specific for the 129 allele; and Nap1L2-Pgk-F (5′-GCACCATCTTTTATCCCCACG-3′), which is specific for the Pgk allele. Both were used in conjunction with a universal reverse primer: Nap1L2-129/Pgk-R (5′-ACAGCAGATGCGCGATGAT-3′). *Nap1L2* cDNA quantitations were standardized against *Rrm2* cDNA (Morey et al., 2004).

RNA FISH and immunostaining

Primary antibodies used have recently been described (Okamoto et al., 2004): rabbit polyclonals detecting H3 acK9, H3 di-meK4, H3 di-meK9 (Upstate biotechnology); mouse monoclonal anti-H3 di/tri-meK27 (7B11); rabbit polyclonal anti-Enx1 (Ezh2); and mouse monoclonal anti-Eed (Sewalt et al., 1998; Hamer et al., 2002). TS and XEN cells cultured on gelatin-coated coverslips were fixed in 3% paraformaldehyde for 15 minutes at room temperature. Permeabilization was performed on ice in PBS containing 0.5% Triton X-100 and 2 mM Vanadyl Ribonucleoside Complex (VRC, Biolabs) for 3.5 minutes. After rinsing in PBS, preparations were blocked in 1% BSA (Gibco) and 0.4 U/ml RNAguard (Amersham/Pharmacia) in PBS for 15 minutes, incubated with primary antibody (diluted in blocking buffer) for 40 minutes, then washed in PBS four times, 5 minutes each, and incubated with secondary antibody (Alexa Fluor 568 goat anti-rabbit or anti-mouse, Molecular Probes) in blocking buffer for 40 minutes at room temperature. After washing in PBS, preparations were post-fixed in 3% paraformaldehyde for 10 minutes at room temperature and rinsed in 2×SSC. For RNA FISH, the *Xist* probe used was a 19 kb genomic fragment derived from a lambda clone (510) that covers most of the *Xist* gene. The probe was labeled by nick translation (Vysis) with spectrum green-dUTP (Vysis), and was hybridized (0.1 mg of probe with 10 mg of salmon sperm DNA per coverslip) in 50% formamide, 2×SSC, 20% dextran sulfate, 1 mg/ml BSA (NEB), 200 mM VRC, overnight at 37°C. After three washes in 50% formamide/2×SSC and three washes in 2×SSC at 42°C, DNA was counterstained for 2 minutes in 0.2 mg/ml DAPI, followed by a final wash in 2×SSC. Samples were mounted in 90% glycerol, 0.1×PBS, 0.1% p-phenylenediamine (Aldrich) (pH 9). A Leica DMR fluorescence microscope with a Cool SNAP fx camera (Photometrics) and Metamorph software (Roper) were used for image acquisition.

Results

Derivation of XEN cell lines

Extra-embryonic endoderm (XEN) cell lines were derived by three different methods in three different laboratories (Table 1). In the first, four XEN cell lines (IM5A1, IM8A1, IM8A2 and IM9C4) were derived from inner cell masses (ICMs) under TS cell derivation conditions (Tanaka et al., 1998). Three additional XEN cell lines (XEN1-2, XEN1-3 and XEN1-4) were derived from wild-type outbred ICR embryos by plating out single blastocysts in the aforementioned conditions. Although FGF4 was used during the derivation process of the above cell lines, this factor is not required for the maintenance of XEN cell cultures and all XEN cell lines grow well in EMFI-conditioned medium. Moreover, the presence of exogenous FGF4 is not essential during the derivation process because a third series of XEN cell lines, GHP7/3, GHP7/9 and GHP7/7, was isolated from E3.5 blastocysts using standard LIF-containing medium without FGF4. Six XEN cell lines have

Table 1. XEN cell lines

XEN cell line	Mouse strain/genotype	Sex	Laboratory
GHP7/3	Tgn (X^{GFP})4 × 129Hprt^{bm1}Pgk1a	F	Avner
GHP7/7	Tgn (X^{GFP})4 × 129Hprt^{bm1}Pgk1a	M	Avner
GHP7/9	Tgn (X^{GFP})4 × 129Hprt^{bm1}Pgk1a	F	Avner
IM5A1	PO strain; ROSA26 βgeo/+	F	Gardner
IM8A1	PO strain; ROSA26 βgeo/+	–	Gardner
IM8A2	PO strain; ROSA26 βgeo/+	–	Gardner
IM9C4	PO strain; ROSA26 βgeo/+	F	Gardner
XEN1-2	ICR strain; wild type	–	Rossant
XEN1-3	ICR strain; wild type	M	Rossant
XEN1-4	ICR strain; wild type	–	Rossant

Summary of the 10 XEN cell lines, indicating their background, sex (where known) and the laboratory where it was derived.

been passaged at least 12 times each without undergoing senescence or a reduction in viability, with one cell line (IM8A1) being passaged more than 50 times (more than 6 months in culture). All XEN cell lines have been cryopreserved and recovered without loss of viability. The sex of two PO XEN cell lines, one ICR XEN cell line and all three of the GHP XEN cell lines was determined by X and Y chromosome-specific PCR. Two of the lines are male (XY: XEN1-3 and GHP7/7) and four are female (XX: IM5A1, IM9C4, GHP7/3 and GHP7/9), demonstrating that there is no restriction on the sex of XEN cells. FACS analysis with propidium iodide determined that the vast majority of XEN cells contain a diploid DNA content with some tetraploid cells. Two GHP XEN cell lines were further characterized for their karyotype, which confirmed the majority of cells were diploid (data not shown). The extent to which these cell lines are chromosomally stable and remain euploid during prolonged culture awaits detailed investigation.

In summary, XEN cell lines can be consistently derived from blastocysts or ICMs from different genetic backgrounds. Derivation from ICMs was more efficient than from intact blastocysts. However, once derived all XEN cell lines could be maintained in EMFI-CM on gelatin without supplementation with additional growth factors.

XEN cell morphology and behavior

In contrast to the coherent colonies formed by ES and TS cells, XEN cells maintain very little cell-cell contact when grown at low density. The cultures contain at least two cell morphologies; a rounded, highly refractile cell type and a more stellate epithelial-like cell type (Fig. 1B). At higher densities XEN cells could form epithelial sheets (Fig. 1C) and often formed a lattice-type structure (Fig. 1D). When XEN cells were removed from gelatin and plated on tissue culture plastic without EMFI-CM, many cells became large and vacuolated within 6 days (Fig. 1E) and the cell lines could no longer be passaged. Although there was some variability observed between different cell lines in terms of proliferation rates and ratios of round versus epithelioid cell types, the basic morphology of the cultures was consistent and easily recognizable.

To investigate whether the presence of the two cell morphologies represented two cell types in the starting cultures, we FACS-sorted single GFP-labeled XEN cells directly into 96-well plates and subclonal cell lines were derived. Cell viability was ~50% and 16% (31/192) of the subclonal cultures could be passaged. Importantly, all subclonal lines exhibited both round and epithelial-like cell morphologies. This suggested that the two cell morphologies observed in the parental cell line was not due to a mixture of

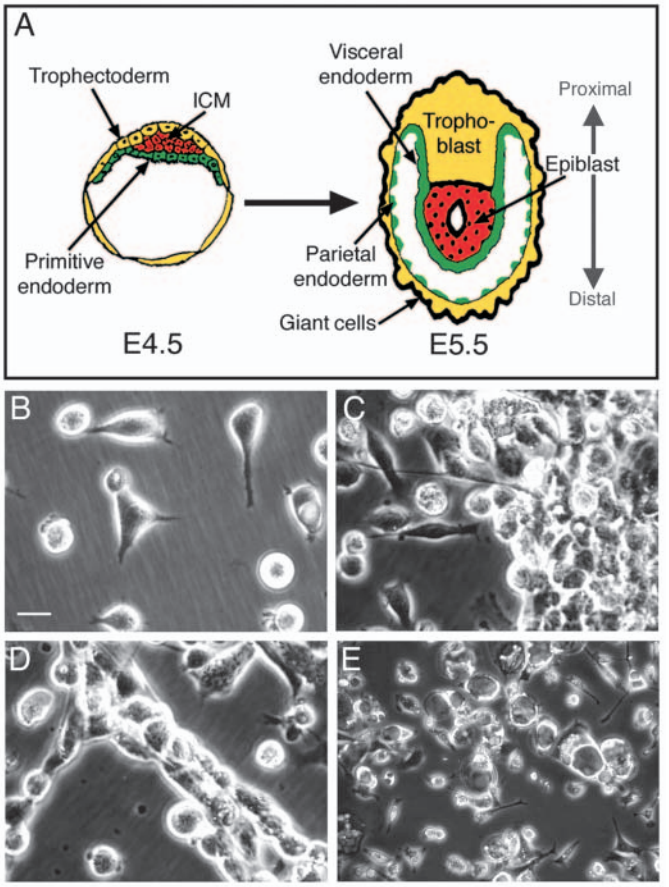

Fig. 1. The extra-embryonic endoderm lineage and XEN cell cultures. (A) Schematic of an E4.5 blastocyst and an E5.5 embryo, illustrating the primitive, visceral and parietal endoderm (green). The trophoblast and epiblast lineages are represented in yellow and red, respectively. The proximodistal axis is indicated. ICM, inner cell mass. (B) Phase-contrast micrograph of XEN cells cultured at low density illustrating the refractile, rounded cell type and the epithelioid cell type. (C) XEN cells grown to near confluency showing the presence of individual cells and an epithelial sheet of cells. (D) XEN cells participating in a lattice-type structure. (E) XEN cells plated in the absence of gelatin resulted in differentiation of some cells into large vacuolated cells in 6 days. Scale bar: 10 μm for B-D; 40 μm for E.

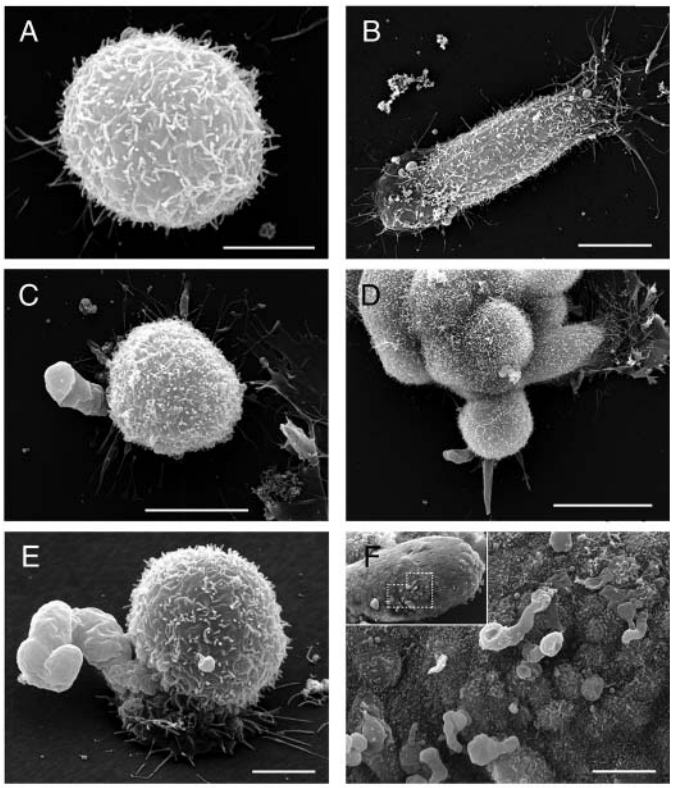

Fig. 2. Scanning electron microscopy of XEN cells and a pre-gastrula embryo. (A) Rounded XEN cell with numerous microvilli. (B) Epithelial-like XEN cell with numerous microvilli and lamellepodia at opposite ends. (C) Isolated XEN cell with a short pseudopodium. (D) Colony of XEN cells where one cell is extending several pseudopodia. (E) Isolated XEN cell with a curving pseudopodium viewed at a 60° angle. This XEN cell is on a pedestal structure and the pseudopodium is originating from below the cell. (F) E5.5 embryo with Reichert's membrane removed (inset) and a higher magnification of the anterior visceral endoderm region (broken line). Scale bars: 5 μm for A,E; 10 μm for B,C,F; 20 μm for D.

two distinct cell populations that were being co-cultured. Videomicroscopy showed that XEN cells are highly motile and that single cells made transitions between round and epithelioid cell types without cell division (see Movie 1 in the supplementary material). Twenty-five individual XEN cells were followed for a 9-hour period by videomicroscopy and 76% (19/25) underwent reversible phenotypic changes (round-to-epithelioid-to-round or epithelioid-round-epithelioid) without cell division. Thus, the two cell morphologies represent different phases of the dynamic behavior of XEN cells in culture.

During these studies, we observed a large, unusual cell process being transiently produced by 25% of XEN cells in their rounded, but not their epithelioid, phase. The cellular process was rapidly extruded and retracted (within 6-10 minutes) and was often longer than a cell diameter and as wide as 30-40% of the thickness of the cell. Scanning electronmicroscopy (SEM) revealed that although both the rounded and epithelioid XEN cell surfaces were very dense with microvilli (Fig. 2A,B), the large pseudopodium was completely devoid of them (Fig. 2C-E). SEM images taken at a 60° angle showed that the pseudopodia were not attached to the cell culture substrate, but were raised above it (Fig. 2E). PE and VE of E5.0-E6.5 embryos were also analyzed by SEM and very similar pseudopodia were found protruding from the distal and anterior VE regions of E5.25-E5.75 embryos (Fig. 2F). These protrusions were not observed on PE cells or other regions of the VE, and disappeared completely by E6.5. Thus, although the overall morphology of the XEN cultures resembles PE, the presence of pseudopodia is a property more typical of VE.

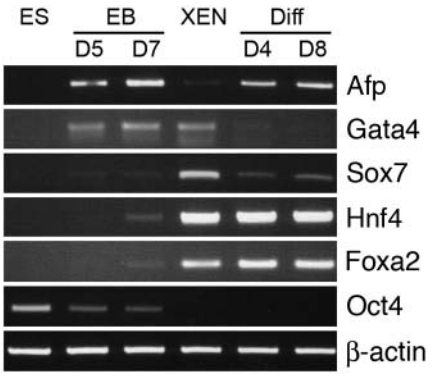

Fig. 3. RT-PCR expression analysis of XEN cells. cDNA was prepared from ES cells, embryoid bodies (EB) at day 5 (D5) and day 7 (D7), and three different XEN cell cultures. XEN cells were either cultured on gelatin in maintenance conditions (XEN) or differentiated (Diff) by removal of EMFI-CM and gelatin for 4 or 8 days (D4, D8). *Hnf4* and *Foxa2* were consistently detected in all XEN cell cultures, while *Gata4* and *Sox7* decreased expression upon differentiation. By contrast, α-fetoprotein (*Afp*) increased with differentiation. *Oct4* was undetectable in XEN cells.

XEN cells express markers of extra-embryonic endoderm

We performed an initial expression analysis of XEN cells by reverse-transcriptase-PCR (RT-PCR) on RNA isolated from XEN cells cultured under maintenance and differentiation conditions. We investigated several known markers of the extra-embryonic endoderm. The VE marker α-fetoprotein (*Afp*) was barely detectable in maintenance cultures, but increased upon differentiation. By contrast, *Gata4* and *Sox7* expression decreased upon differentiation, while *Hnf4* and *Foxa2* levels remained constant (Fig. 3).

XEN cell lines were further characterized by microarray gene expression analysis of three biological replicates. In order to identify genes that were consistently expressed, irrespective of background or culture medium, the replicates were chosen to provide samples from different mouse strains under different culture conditions. The XEN cell cultures were: (1) XEN1-3 cells (ICR strain, passage 18) grown on gelatin with EMFI-CM (sample 'XEN1-3′); (2) IM8A1 cells (PO strain, passage 27) cultured as above (sample 'IM8A1-I'); and (3) IM8A1 cells (passage 27) grown on tissue culture plastic without EMFI-CM for 4 days (sample 'IM8A1-II'). The third sample (IM8A1-II), grown in differentiation conditions, exhibited some morphological changes, such as larger cells, but vacuolated cells were not present. The mouse U74Av2 Affymetrix array was used for this analysis. A fourth sample, undifferentiated

ES cells, was also analyzed on the same array. Data were analyzed for expression of specific marker genes of visceral and parietal endoderm and genes characteristic of ES and TS cells (Table 2). Signaling pathways, selected gene families and transcription factors involved in early development were also analyzed in this manner (see Table S2 in the supplementary material).

Genes specifically expressed in parietal endoderm alone, and not in visceral endoderm or markers common to both lineages were highly expressed in XEN cells (Table 2). Extracellular matrix (ECM) proteins expressed by parietal endoderm to make Reichert's membrane were also abundant. Perlecan (heparin sulfate proteoglycan 2), type IV collagen (α1 and α2 chains only), *laminin* (α1, β1, and β2 chains), and nidogens 1 and *2* (Hogan et al., 1980; Semoff et al., 1982) were expressed in all XEN cell samples (see Table S2 in the supplementary material).

Several genes implicated, by mutant analysis, in visceral endoderm function were also expressed in XEN cells. These genes are, however, are also expressed in primitive and parietal endoderm and may be more representative of primitive endoderm. They include *Gata4* and *Gata6* (Arceci et al., 1993; Koutsourakis et al., 1999; Narita et al., 1997), *Disabled2* (Morris et al., 2002; Yang et al., 2002), *Tcf2* (*vHnf1*) (Barbacci et al., 1999) and *Vegfa* (Miquerol et al., 1999). Markers specific to VE are often difficult to identify because of the lack of comparable expression data for parietal endoderm. From published expression data where both PE and VE were investigated, several VE-specific genes have been identified. A number of these genes were expressed in XEN cells and they include *Foxa2* (Dufort et al., 1998), *Ihh* (Becker et al., 1997) and type I Acvr1 (Gu et al., 1999). Other VE-specific genes, such as *Afp*, *Hnf4* and *uPA* (*Plau*) were not detected (Table 2). However, *Afp* can be induced in differentiated XEN cell

Table 2. Expression of known genes in XEN cells

Affy ID	Unigene	Gene name or symbol	XEN1-3	IM8A1-I	IM8A1-II	Reference
PE genes						
100717_at	Mm.2093	*Snail*	590	660	239	Veltmaat et al., 2000
95079_at	Mm.221403	*Pdgfra*	1057	1487	1056	Mercola et al., 1990
104601_at	Mm.24096	Thrombomodulin	219	393	199	Healy et al., 1995
93981_at	Mm.154660	tPA, tissue-type plasminogen activator	1641	1893	1191	Marotti et al., 1982
98482_at	Mm.3542	*Pthr1*	2276	2128	1384	Verheijen et al., 1999a
98817_at	Mm.4913	Follistatin	1869	3475	2990	Feijen et al., 1994
97160_at	Mm.291442	*Sparc*	5924	7284	7376	Mason et al., 1986
VE genes						
93950_at	Mm.938	*Foxa2* (Hnf3β)	552	512	520	Dufort et al., 1998
160705_at	Mm.2390	*Cited1* (Msg1)	1208	1032	1651	Dunwoodie et al., 1998
103949_at	Mm.2543	Indian hedgehog (*Ihh*)	182	63	156	Becker et al., 1997
98320_at	Mm.42230	*Cyp26a1* (*P450RAI*)	354	1721	1010	Fujii et al., 1997
100515_at	Mm.5241	*Furin*	450	327	455	Roebroek et al., 1998
93460_at	Mm.689	*Acvr1*, Activin A receptor, type 1	93	65	64	Gu et al., 1999
92713_at	Mm.202383	*Hnf4*	A	A	A	Duncan et al., 1994
101493_at	Mm.358570	*Afp*, α-fetoprotein	A	A	A	Dziadek and Adamson, 1978
101494_at	Mm.358570	*Afp*, α-fetoprotein	A	A	A	Dziadek and Adamson, 1978
97772_at	Mm.4183	*Plau*, plasminogen activator, urokinase	A	A	A	Marotti et al., 1981
PE and VE genes						
102713_at	Mm.247669	*Gata4*	1091	1196	899	Arceci et al., 1993
104698_at	Mm.329287	*Gata6*	2468	1973	1086	Koutsourakis et al., 1999
92487_at	Mm.42162	*Sox7*	981	1339	225	Kanai-Azuma et al., 2002
92997_g_at	Mm.279103	*Sox17*	1024	1436	1285	Kanai-Azuma et al., 2002
92996_at	Mm.279103	*Sox17*	1293	1895	1712	Kanai-Azuma et al., 2002
101396_at	Mm.7226	*Dab2*, *Tcf2* (*vHnf1*)	111	189	138	Barbacci et al., 1999
98044_at	Mm.240830	Disabled2	206	277	624	Yang et al., 2002
102258_at	Mm.10801	*Stra6*	465	296	85	Bouillet at al., 1997
103520_at	Mm.282184	*Vegfa*	112	263	158	Miquerol et al., 1999
101009_at	Mm.358618	Krt2-8 (Endo A)	1358	1962	2737	Hashido et al., 1991
94270_at	Mm.22479	Krt1-18 (Endo B)	1192	2104	3834	Oshima, 1981
ES and TS cell genes						
103075_at	Mm.17031	*Pou5f1* (*Oct4*)	A	A	A	Palmieri et al., 1994
161072_at	Mm.6047	*Nanog*	A	A	A	Wang et al., 2003
98414_at	Mm.285848	*Zfp42* (Rex1)	A	A	A	Rogers et al., 1991
93880_at	Mm.200692	*Eomes*, Eomesodermin	A	A	A	Tanaka et al., 1998
103532_at	Mm.200692	*Eomes*, Eomesodermin	A	A	A	Tanaka et al., 1998
100301_at	Mm.235550	*Esrrb*, Errβ	A	A	A	Tanaka et al., 1998
103239_at	Mm.20358	*Cdx2*	A	A	A	Tanaka et al., 1998

A subset of genes from expression analysis of XEN cells by Affymetrix profiling (from the mouse U74Av2 Affymetrix array). Data are shown for genes known to be expressed in the VE, PE and other embryonic lineages. The Affy Clone ID, Unigene designation and gene name or symbol are listed. The three XEN samples (XEN1-3, IM8A1-I and IM8A1-II) are described in the text. If a gene is expressed at statistically significant levels ($P<0.04$), its expression level is indicated by a numerical value; if a gene is not expressed, it is indicated by 'A' (absent). A single reference is provided for each gene and others are mentioned in the text. The groupings are a rough guide, as PE expression data for many genes are not available. In addition, many of these genes are expressed at other stages and tissues during development.

Table 3. XEN cell chimera data

XEN cells	Stage	Number transferred	Number of embryos	Number of chimeras
Population	E6.5	34	30	8
	E7.5	36	23	8
	E8.5	42	25	7
Clone 4	E6.5	42	27	13
	E7.5	42	30	10
	E8.5	41	33	4
Total	E6.5-E8.5	237	168 (71%)	50 (30%)

GFP-IM8A1 XEN cells (FACS-sorted population) and a subclonal line, GFP-IM8A1-4 (Clone 4), were used to generate chimeras by blastocyst injection. The stage dissected, the number of blastocysts transferred, the number of embryos recovered and the number of chimeras observed are indicated.

cultures and *Hnf4* is indeed detectable by RT-PCR (Fig. 3). Genes representative of TS cells, *Cdx2*, *Eomes* and *Esrrb* (Tanaka et al., 1998), and the ES cell markers, *Oct4*, *Nanog* and *Rex1*, were not detected in XEN cells (Table 2). We conclude, based on our marker studies, that XEN cells derive from the primitive endoderm of the blastocyst and represent derivatives of this lineage.

As well as examining the expression of known extra-embryonic endoderm markers, we also used a comparison of ES cell and XEN cell Affymetrix expression data to seek those genes specifically enriched in XEN cells. The three XEN cell data sets described above were each compared with a single data set from undifferentiated ES cells and three expression ratios were obtained for each gene. These ratios were averaged and rank-ordered, starting with the largest ratio. Within the list of 40 genes with the highest positive expression ratios, at least 13 genes are known extra-embryonic endoderm markers (see Table S3 in the supplementary material). This was in contrast to the list of genes with the largest negative expression ratios, which was highly enriched with known ES cell-specific genes (see Table S4 in the supplementary material).

XEN cell chimeras

We investigated the developmental potential of XEN cells by generating chimeras with a GFP/*lacZ* cell line and one of its subclonal derivatives (Table 3). XEN cells (10-15) were injected into wild-type ICR blastocysts and analyzed for contributions at E6.5, E7.5 and E8.5. GFP/*lacZ* XEN cells were never found to contribute to the embryo proper, yolk sac mesoderm or the trophoblast lineage. The overwhelming number of chimeras (49/50) had XEN cell contributions restricted to parietal endoderm. At E6.5, XEN cells were usually observed as dispersed cells lining the distal part of the parietal yolk sac (Fig. 4A,B). At later stages, chimeras could be found with large numbers of scattered XEN cells in their parietal yolk sacs (Fig. 4C-E). This pattern was typical of parietal endoderm growth in vivo (Hogan and Newman, 1984). A single chimera exhibited a contribution of XEN cells in the visceral endoderm layer (Fig. 4F), but not in the parietal yolk sac (not shown). The nature of this clone was very different from the contributions to the parietal region, as the XEN cells formed a coherent epithelial sheet without intermingling with host cells. This is consistent with the coherent growth characteristics of VE in vivo (Gardner and Cockroft, 1998).

Imprinted X chromosome inactivation in XEN cells

The evidence that XEN cell lines represent cells of the extra-embryonic endoderm lineage led us to analyze the X-inactivation status of female XEN cell lines. If X-inactivation has yet to occur, *Xist* expression should be low from both the maternal and paternal X chromosomes. If imprinted X-inactivation, which appears to onset very early in mouse embryogenesis (Okamoto et al., 2004), has already occurred, *Xist* expression would be expected to be associated with silencing of genes on the paternally inherited X chromosome. Our studies concentrated on the GHP7/9 and GHP7/3 cell lines that are heterozygous for the $Hprt^{bm1}$ mutation and have a maternal X-linked GFP transgene. They also carry polymorphisms for X-linked genes, such as *Xist* and *Nap1l2*. We first addressed whether an inactive X chromosome was present and whether it was subject to imprinting. We used allelic quantitative RT-PCR to assess whether *Xist* and *Nap1l2*

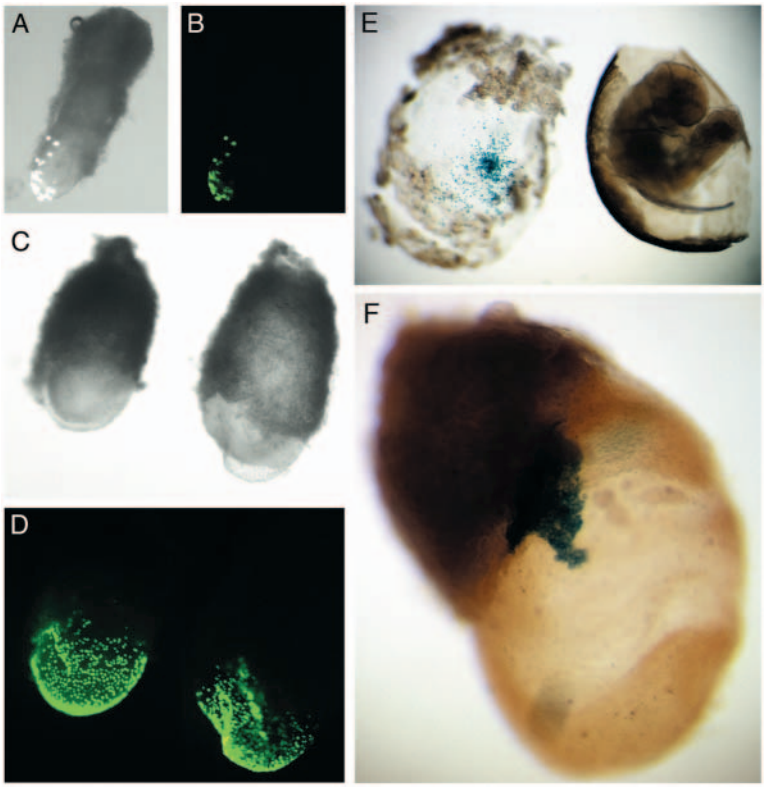

Fig. 4. XEN cell chimeras. (A,B) E6.5 chimera with XEN cells contributions to the distal region of the conceptus in the parietal yolk sac: (A) Partial phase-contrast and UV fluorescence micrograph; (B) UV fluorescence micrograph with false-color added. (C,D) Two E7.5 chimeras with XEN cell contributions exclusively to the parietal yolk sac; phase-contrast (C) and UV fluorescence micrographs (D). (E) E8.5 XEN cell chimera in which the parietal yolk sac was dissected from the visceral yolk sac and embryo proper after X-gal staining. All the X-gal-positive cells were located in the parietal yolk sac and not in other tissues. (F) E7.5 XEN cell chimera after X-gal staining. A coherent XEN cell clone was observed in the extra-embryonic region of the visceral endoderm.

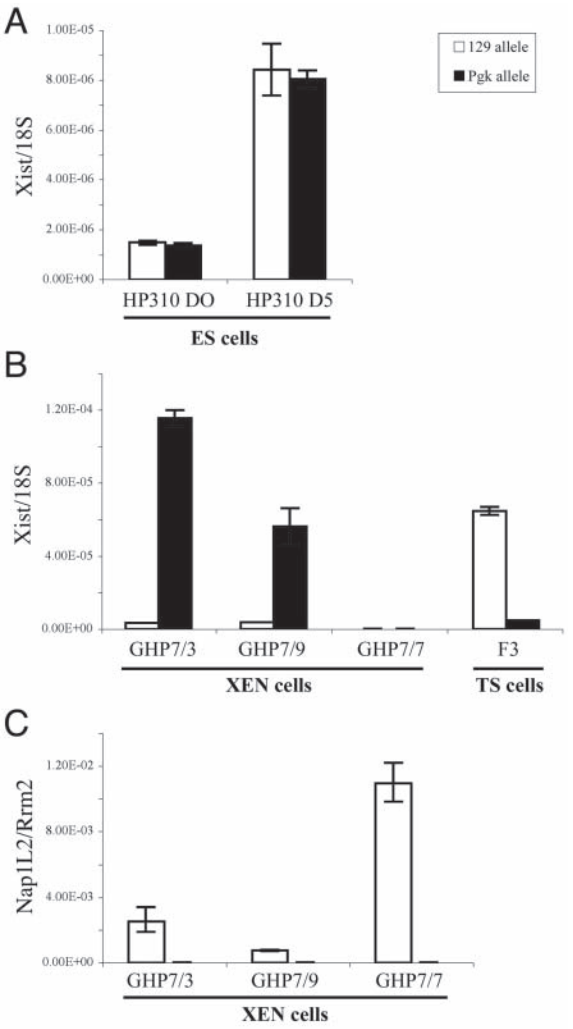

Fig. 5. X-inactivation in ES, TS and XEN cells. Quantification of *Xist* transcripts by real-time RT-PCR in (A) ES cells and (B) XEN and TS cells normalized using the endogenous gene *18S*. (C) Quantification of *Nap1l2* transcripts normalized using the *Rrm2* gene in XEN cells. In differentiated ES cells (A), random X-inactivation leads to equivalent levels of *Xist* expression from the 129 and Pgk alleles. By contrast, in female XEN cells (GHP7/3 and GHP7/9), *Xist* is expressed only from the paternal Pgk allele (B) and *Nap1l2* only from the maternal 129 allele (C), indicating that the paternal X chromosome is preferentially inactivated in female XEN cells, just as in female TS cells (where *Xist* is expressed only from the paternal 129 allele; B). In control male XEN cells (GHP7/7), the single X chromosome derived from 129 is active, as shown by the absence of *Xist* (B) and presence of *Nap1l2* expression (C).

were expressed from the maternal or the paternal X chromosome. In undifferentiated female ES cells, *Xist* expression was low and similar for both parental X chromosomes. The equal increase of maternal and paternal *Xist* expression in differentiated ES cells is indicative of random X-inactivation (Fig. 5A). By contrast, in female XEN cell lines *Xist* expression was overwhelmingly of the 'Pgk' allelic form that corresponds to the paternal allele and was absent from the male GHP7/7 XEN cell line (Fig. 5B). TS cells, harboring a '129' paternal *Xist* allele showed a similar pattern of expression. In agreement with this, uniparental *Nap1l2* expression indicated the presence of an active maternal X chromosome in XEN cells (Fig. 5C). Quantitative RT-PCR analysis of GFP expression, although variable, showed that GFP expression was at least eightfold greater in the female GHP7/3 and GHP7/9 cell lines carrying a maternally inherited X-linked GFP transgene, than in control TS cell lines carrying a paternally inherited X-linked GFP transgene (data not shown). We conclude that the paternal X chromosome expressing *Xist* was chosen to be inactivated in female XEN cell lines.

Growth of XEN cell lines on HAT and 6-thioguanine (6TG) media allows for a more global assessment of stability of the inactive X chromosome by assaying for the presence or absence of a functional *Hprt* gene. The GHP7/9 XEN cell line carrying a functional *Hprt* gene on the maternal X and a non-functional $Hprt^{bm1}$ allele on the paternal X grew on HAT medium and failed to grow on 6TG medium (data not shown). These results support the idea that the paternally inherited X chromosome carrying the mutated allele was inactivated and that the inactivation state is stable in long-term cultures.

When RNA FISH was carried out on female XEN cells, a Xist domain was found in the majority of cells analyzed (Fig. 6A). A pinpoint signal was not found to be associated with the active X chromosome and neither domain nor pinpoint Xist signals were found in the male XEN cell line (GHP7/7). Chromatin modifications associated with the inactive X chromosome in females were examined by Immuno-RNA FISH in female XEN cells. Female TS cell lines were concurrently examined to explore possible differences between the two extra-embryonic lineages. Unlike TS cells, which show an enrichment of Eed and Ezh2 (Mak et al., 2002), the Xist domain in XEN cells show no enrichment for these polycomb group proteins (compare Fig. 6A with 6B). Histone H3 dimethylated K4 (H3 di-meK4), which is normally associated with active euchromatin, is excluded from the Xist domain in both XEN and TS cells, as is histone H3 acetylated K9 (H3 acK9) (Fig. 6; see Fig. S1 in the supplementary material). Histone H3 di-meK9, which has been associated with the inactive X chromosome in differentiating ES cells and somatic cells (Heard et al., 2001), appears only weakly enriched, if at all, in XEN and TS cells (see Fig. S1 in the supplementary material). Histone H3 tri-meK27, which has recently also been associated with the inactive X in both TS cells and differentiating ES cells (Silva et al., 2003), is enriched over the Xist domain in only a small proportion of XEN cells. This is consistent with the absence or low levels of Ezh2 on the X chromosome in XEN cells, as Ezh2 is thought to be the histone methyltransferase responsible for the H3 tri-meK27 mark (Erhardt et al., 2003). Thus, XEN cells exhibit a unique combination of histone modifications on their inactive X chromosome – which includes hypoacetylation of H3 K9, hypomethylation of H3 K4 and little or no methylation of H3 K27 and K9. The stability of the inactive state of the X chromosome in these cells, despite the absence of H3 K9 and H3 K27 methylation, suggests that other epigenetic marks are involved. This is different from the situation in ES cells, where the lack of Ezh2 accumulation and H3 K27 methylation results in significant reactivation of X-linked genes (Silva et al., 2003).

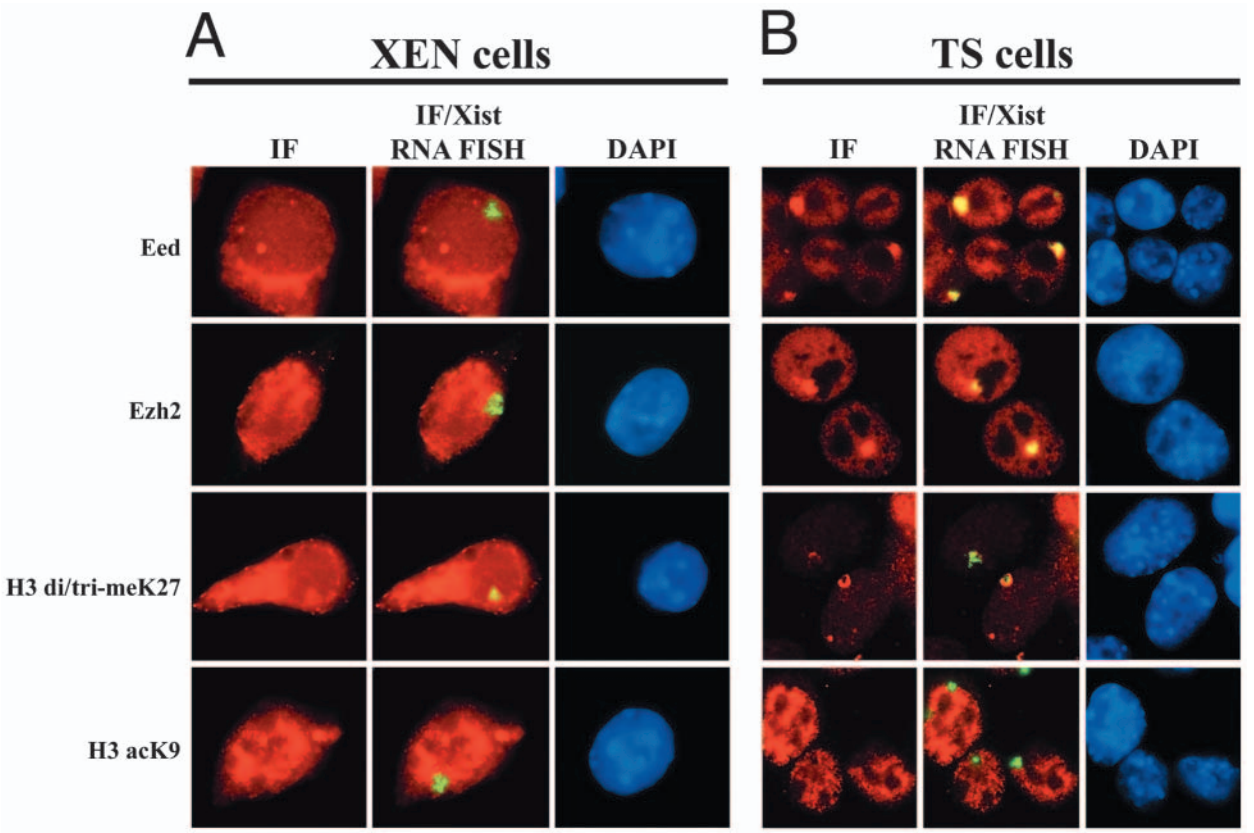

Fig. 6. Histone modifications and *Xist* accumulation in female XEN and TS cells. (A,B) Representative images show immunofluorescent detection of Eed, Ezh2 and histone modifications H3 di/tri-methyl K27 and H3 acetyl K9, combined with *Xist* RNA FISH. Immunodetections were performed using Alexa 568-conjugated secondary antibodies (red). *Xist* RNA was detected using a Spectrum Green-labeled FISH probe (green). XEN cells (A) show no Eed and Ezh2 enrichment, and weak H3 di/tri-meK27 enrichment on the *Xist*-coated X chromosome, but they do show depletion for H3 acK9. By contrast, undifferentiated TS cells (B) show enrichment for Eed, Ezh2 and H3 di/tri-meK27 on the *Xist*-coated X chromosome. Depletion for H3 acK9 was observed, as in XEN cells.

Discussion

We have derived and characterized a number of independent cell lines from mouse blastocysts that exhibit extra-embryonic endoderm characteristics. This ex vivo model, which is reproducibly derived from early embryos, is distinct from ES and TS cell lines. We show here that XEN cells exhibit mixed characteristics of parietal endoderm and visceral endoderm, and can contribute to both lineages in chimeras in vivo, although they are biased towards parietal endoderm. We also show that they exhibit paternal X-inactivation, but without the association of Eed and Ezh2 that typifies the inactive X in TS cells.

XEN cell maintenance

XEN cell cultures are robust and easily maintained, but their precise signaling requirements are not known. After derivation, they can be grown on gelatin in medium supplemented with EMFI-CM. The FGF signaling pathway required for TS cells is not important for XEN cell maintenance and indeed none of the four FGF receptors is expressed in XEN cells (see Table S2 in the supplementary material). The LIF-STAT pathway may be playing a role in XEN cell maintenance. Several components (LIFR, gp130, JAK1, JAK2, STAT1 and STAT3) of this pathway are expressed in XEN cells (see Table S2 in the supplementary material), and their derivation and maintenance on EMFIs or EMFI-CM would provide an adequate source of LIF (Smith et al., 1992).

XEN cells show properties of both parietal and visceral endoderm

The previously reported mouse PEC and rat RE1 cell lines are similar, if not identical, to the XEN cells described here. The two distinct morphologies of XEN cells in culture – rounded highly refractile and flattened epithelioid – have also been reported (Fowler et al., 1990; Notarianni and Flechon, 2001). These cell lines are considered representative of parietal endoderm based on their morphology and the secretion of ECM proteins abundantly found in Reichert's membrane. Our Affymetrix expression analysis of XEN cells supports the idea that PE properties are highly represented in such cell culture models. PE-associated genes, such as *tPA* (*Plat*), thrombomodulin, *Snail* and *Pdgfra*, were strongly expressed. Genes encoding for basement membrane proteins (perlecan, type IV collagen, laminin and nidogen), abundant in Reichert's membrane, were also expressed at high levels in XEN cells.

XEN cells, however, also expressed several VE-associated genes in all cultures (Table 2). The high expression of *Sox7*, *Sox17* and *Cited1* were of particular interest, given their

restricted expression in VE overlying the extra-embryonic ectoderm and in the marginal zone VE (Dunwoodie et al., 1998; Kanai-Azuma et al., 2002). The reduction of *Sox7* and increase of *Afp* expression in differentiated XEN cell cultures suggests that XEN cells may have some properties of extra-embryonic VE when cultured in standard conditions, but can be differentiated to cells more related to the VE overlying the epiblast in other conditions. Furthermore, *Sox7* expression suggests that definitive endoderm is not present in XEN cell cultures, as this gene, unlike *Sox17*, is not detectable in definitive endoderm in vivo (Kanai-Azuma et al., 2002).

The single-cell clonal analysis and videomicroscopy studies of XEN cells have indicated that the rounded and epithelial-like cell types are lineage-related and reversibly interchangeable. The morphology of marginal zone VE cells in vivo is similar to the flattened, epithelial-like cells observed in culture. The marginal zone cells have been described as mesenchymal with ruffled cell membranes reminiscent of lamellipodia (Hogan and Newman, 1984). The unusual pseudopodia we observed in XEN cells were also observed in the AVE region of early postimplantation embryos in vivo (Fig. 2F), suggesting that XEN cells may also transiently become AVE like. Taken together, the gene expression studies and cell morphology/behavior suggest that clonal XEN cell cultures exhibit properties of PE, marginal zone VE, AVE and extra-embryonic VE, but not of embryonic VE. However, the induction of an embryonic VE marker, *Afp*, in differentiated cultures of XEN cells (Fig. 3) suggests that this VE subtype could be induced in defined conditions.

XEN cell chimeras

XEN cell lines retain the capacity to contribute to primitive endoderm derivatives in vivo in chimeras, attesting to their primitive endoderm nature and the stability of their ex vivo phenotype. However, they exhibited a strong bias to form parietal endoderm in chimeras, with only one visceral endoderm clone observed. This does not necessarily indicate their full potential. The blastocyst injection procedure used to generate chimeras may have provided an environment that promotes PE and hinders VE differentiation. XEN cells injected into the blastocoel are likely to end up in the superficial layer of the primitive endoderm as it forms (Gardner, 1985) or associated with the TE away from the ICM. PrE or VE cells that lose contact with epiblast and extra-embryonic ectoderm default to a PE phenotype or are instructed by the trophectoderm to become PE by a combination of TE basement membrane and the PTHrP/cAMP signaling pathway (Verheijen et al., 1999a). This observation is supported by chimera experiments with primitive endoderm cells and nascent VE cells directly isolated from embryos. Blastocyst injection of PrE or early VE cells also resulted in chimeras with mostly PE contributions (Gardner, 1982; Cockroft and Gardner, 1987). Although the donor PrE and VE cells clearly have the potential to make VE, their behavior in chimeras did not reflect this. Given this intrinsic bias, an alternative method for producing chimeras, such as morula or ICM injections, may be required to observe the full potential of XEN cells.

Imprinted X-inactivation in XEN cells

The extra-embryonic trophoblast and endoderm lineages of the mouse undergo imprinted inactivation of the paternal X chromosome (Xp) (Takagi and Sasaki, 1975). Initiation of X inactivation requires expression of the non-coding RNA, *Xist*, and accumulation of this transcript on the inactive X chromosome in cis (Penny et al., 1996). In agreement with their proposed extra-embryonic endodermal origin, XEN cells maintain imprinted X inactivation of the Xp and exhibit *Xist* accumulation on one X chromosome. This Xist domain also exhibits other epigenetic marks of being inactive, such as exclusion of histone H3 acetylated K9 and dimethylated K4, both hallmarks of active euchromatin (Heard et al., 2001; Boggs et al., 2002). Surprisingly, accumulation of the polycomb group proteins, Eed and Ezh2, was not observed in XEN cells, as is seen in TS cells (Fig. 6) (Mak et al., 2002). Mutant analysis revealed an important role for *Eed* in the formation of trophoblast giant cells, but not extra-embryonic endoderm, during development (Wang et al., 2002). The proposed substrate of Ezh2, histone H3 K27, appears to be weakly di/trimethylated in some XEN cells, suggesting a transient association of Ezh2. Thus, the mechanisms to maintain X inactivation in XEN cells, TS cells and ES cells differ at the levels of polycomb group proteins and histone modifications. The HAT/6TG studies indicate that the inactive state of the Xp in XEN cells is stable, despite the absence of H3 meK9 enrichment and low levels of H3 K27 methylation. This suggests XEN cells may have different mechanisms for maintenance of their inactive X chromosome and that other epigenetics marks likely account for the stability of the inactive state. These results illustrate the cell lineage-dependent variation in mechanisms of X-inactivation maintenance that has also been observed in other systems (Plath et al., 2003).

XEN cells from ES cells

The XEN cell lines described here were derived de novo from blastocysts. However, two reports suggest that similar cell lines can be derived directly from established ES cell lines. Overexpression of the GATA factors, GATA4 or GATA6, in ES cells induced uniform differentiation into extra-embryonic endoderm cells (Fujikura et al., 2002). In terms of marker analysis and cell morphology, these cells appear identical to XEN cells. Fujikura et al., hypothesize that a repressor of *Gata4/6* expression is required to maintain ES cells pluripotent. The recently identified pluripotent transcription factor, Nanog, may fulfill this role (Chambers et al., 2003; Mitsui et al., 2003). *Nanog*$^{-/-}$ ES cells express many markers of extra-embryonic endoderm (*Gata6*, *Tcf2* and *Ihh*) and are also morphologically very similar to XEN cells (Mitsui et al., 2003). This implicates Nanog as a general repressor of the extra-embryonic endoderm lineage and it may function, in part, through repression of key regulatory genes, such as *Gata6*.

XEN cell lines provide a unique model for an early mammalian lineage that will complement the established ES and TS cell lines. Through the study of essential genes and signaling requirements for this cell culture system, insights will be gained about the developmental program of the extra-embryonic endoderm lineage. In addition, in vitro combinations of ES, TS and XEN cells may help model the in vivo interactions between embryonic and extra-embryonic lineages important for embryonic patterning.

We gratefully acknowledge the assistance of Doug Holmyard for scanning electron microscopy, Feng Xu for videomicroscopy, Brian Cox for Affymetrix data processing, Claude Cantin for FACS, Sandra Tondat for blastocyst injections, Sylvain Pichard and Constance Ciaudo for technical work, and José Silva and Pleasantine Mill for critical discussions. We thank Arie Otte and Danny Reinberg for the kind gift of antibodies. G.D.U. acknowledges the Natural Sciences and Engineering Council of Canada for a postgraduate scholarship. R.L.G. is funded by the Royal Society. E.H. and I.O. were financed by the French Ministry of Research, under the Action Concertée Incitative (ACI), contract number 032515. P.A. was financed by the French Ministry of Research under the ACI, contract number 032526 and the Association pour la Recherche sur le Cancer. T.K. and J.R. were funded by the Canadian Institutes of Health Research (CIHR). J.R. is a CIHR Distinguished Investigator.

Supplementary material

Supplementary material for this article is available at
http://dev.biologists.org/cgi/content/full/132/7/1649/DC1

References

Ang, S. L., Conlon, R. A., Jin, O. and Rossant, J. (1994). Positive and negative signals from mesoderm regulate the expression of mouse Otx2 in ectoderm explants. *Development* **120**, 2979-2989.

Arceci, R. J., King, A. A., Simon, M. C., Orkin, S. H. and Wilson, D. B. (1993). Mouse GATA-4: a retinoic acid-inducible GATA-binding transcription factor expressed in endodermally derived tissues and heart. *Mol. Cell. Biol.* **13**, 2235-2246.

Barbacci, E., Reber, M., Ott, M. O., Breillat, C., Huetz, F. and Cereghini, S. (1999). Variant hepatocyte nuclear factor 1 is required for visceral endoderm specification. *Development* **126**, 4795-4805.

Becker, S., Wang, Z. J., Massey, H., Arauz, A., Labosky, P., Hammerschmidt, M., St-Jacques, B., Bumcrot, D., McMahon, A. and Grabel, L. (1997). A role for Indian hedgehog in extraembryonic endoderm differentiation in F9 cells and the early mouse embryo. *Dev. Biol.* **187**, 298-310.

Biben, C., Stanley, E., Fabri, L., Kotecha, S., Rhinn, M., Drinkwater, C., Lah, M., Wang, C. C., Nash, A., Hilton, D. et al. (1998). Murine cerberus homologue mCer-1: a candidate anterior patterning molecule. *Dev. Biol.* **194**, 135-151.

Boggs, B. A., Cheung, P., Heard, E., Spector, D. L., Chinault, A. C. and Allis, C. D. (2002). Differentially methylated forms of histone H3 show unique association patterns with inactive human X chromosomes. *Nat. Genet.* **30**, 73-76.

Bouillet. P., Sapin. V., Chazaud, C., Messaddeq, N., Décimo, D., Dollé, P. and Chambon, P. (1997). Developmental expression pattern of Stra6, a retinoic acid-responsive gene encoding a new type of membrane protein. *Mech. Dev.* **63**, 173-186.

Byrd, N., Becker, S., Maye, P., Narasimhaiah, R., St-Jacques, B., Zhang, X., McMahon, J., McMahon, A. and Grabel, L. (2002). Hedgehog is required for murine yolk sac angiogenesis. *Development* **129**, 361-372.

Chambers, I., Colby, D., Robertson, M., Nichols, J., Lee, S., Tweedie, S. and Smith, A. (2003). Functional expression cloning of Nanog, a pluripotency sustaining factor in embryonic stem cells. *Cell* **113**, 643-655.

Clerc, P. and Avner, P. (1998). Role of the region 3′ to Xist exon 6 in the counting process of X-chromosome inactivation. *Nat. Genet.* **19**, 249-253.

Cockroft, D. L. and Gardner, R. L. (1987). Clonal analysis of the developmental potential of 6th and 7th day visceral endoderm cells in the mouse. *Development* **101**, 143-155.

Coucouvanis, E. and Martin, G. R. (1999). BMP signaling plays a role in visceral endoderm differentiation and cavitation in the early mouse embryo. *Development* **126**, 535-546.

Damert, A., Miquerol, L., Gertsenstein, M., Risau, W. and Nagy, A. (2002). Insufficient VEGFA activity in yolk sac endoderm compromises haematopoietic and endothelial differentiation. *Development* **129**, 1881-1892.

Dickson, A. D. (1979). The disappearance of the decidua capsularis and Reichert's membrane in the mouse. *J. Anat.* **129**, 571-577.

Dufort, D., Schwartz, L., Harpal, K. and Rossant, J. (1998). The transcription factor HNF3beta is required in visceral endoderm for normal primitive streak morphogenesis. *Development* **125**, 3015-3025.

Duncan, S. A., Manova, K., Chen, W. S., Hoodless, P., Weinstein, D. C., Bachvarova, R. F. and Darnell, J. E. Jr (1994). Expression of transcription factor HNF-4 in the extraembryonic endoderm, gut, and nephrogenic tissue of the developing mouse embryo: HNF-4 is a marker for primary endoderm in the implanting blastocyst. *Proc. Natl. Acad. Sci. USA* **91**, 7598-7602.

Dunwoodie, S. L., Rodriguez, T. A. and Beddington, R. S. (1998). Msg1 and Mrg1, founding members of a gene family, show distinct patterns of gene expression during mouse embryogenesis. *Mech. Dev.* **72**, 27-40.

Dyer, M. A., Farrington, S. M., Mohn, D., Munday, J. R. and Baron, M. H. (2001). Indian hedgehog activates hematopoiesis and vasculogenesis and can respecify prospective neurectodermal cell fate in the mouse embryo. *Development* **128**, 1717-1730.

Dziadek, M. (1978). Modulation of alphafetoprotein synthesis in the early postimplantation mouse embryo. *J. Embryol. Exp. Morphol.* **46**, 135-146.

Dziadek, M. and Adamson, E. (1978). Localization and synthesis of alphafoetoprotein in post-implantation mouse embryos. *J. Embryol. Exp. Morphol.* **43**, 289-313.

Enders, A. C., Given, R. L. and Schlafke, S. (1978). Differentiation and migration of endoderm in the rat and mouse at implantation. *Anat. Rec.* **190**, 65-77.

Erhardt, S., Su, I. H., Schneider, R., Barton, S., Bannister, A. J., Perez-Burgos, L., Jenuwein, T., Kouzarides, T., Tarakhovsky, A. and Surani, M. A. (2003). Consequences of the depletion of zygotic and embryonic enhancer of zeste 2 during preimplantation mouse development. *Development* **130**, 4235-4248.

Evans, M. J. and Kaufman, M. H. (1981). Establishment in culture of pluripotential cells from mouse embryos. *Nature* **292**, 154-156.

Feijen, A., Goumans, M. J. and van den Eijnden-van Raaij, A. J. (1994). Expression of activin subunits, activin receptors and follistatin in postimplantation mouse embryos suggests specific developmental functions for different activins. *Development* **120**, 3621-3637.

Fowler, K. J., Mitrangas, K. and Dziadek, M. (1990). In vitro production of Reichert's membrane by mouse embryo-derived parietal endoderm cell lines. *Exp. Cell. Res.* **191**, 194-203.

Fujii, H., Sato, T., Kaneko, S., Gotoh, O., Fujii-Kuriyama, Y., Osawa, K., Kato, S, and Hamada, H. (1997). Metabolic inactivation of retinoic acid by a novel P450 differentially expressed in developing mouse embryos. *EMBO J.* **16**, 4163-4173.

Fujikura, J., Yamato, E., Yonemura, S., Hosoda, K., Masui, S., Nakao, K., Miyazaki Ji, J. and Niwa, H. (2002). Differentiation of embryonic stem cells is induced by GATA factors. *Genes Dev.* **16**, 784-789.

Gardner, R. L. (1982). Investigation of cell lineage and differentiation in the extraembryonic endoderm of the mouse embryo. *J. Embryol. Exp. Morphol.* **68**, 175-198.

Gardner, R. L. (1985). Regeneration of endoderm from primitive ectoderm in the mouse embryo: fact or artifact? *J. Embryol. Exp. Morphol.* **88**, 303-326.

Gardner, R. L. and Cockroft, D. L. (1998). Complete dissipation of coherent clonal growth occurs before gastrulation in mouse epiblast. *Development* **125**, 2397-2402.

Gu, Z., Reynolds, E. M., Song, J., Lei, H., Feijen, A., Yu, L., He, W., MacLaughlin, D. T., van den Eijnden-van Raaij, J., Donahoe, P. K. and Li, E. (1999). The type I serine/threonine kinase receptor ActRIA (ALK2) is required for gastrulation of the mouse embryo. *Development* **126**, 2551-2561.

Hadjantonakis, A.-K., Gertsenstein, M., Ikawa, M., Okabe, M. and Nagy, A. (1998). Generating green fluorescent mice by germline transmission of green fluorescent ES cells. *Mech. Dev.* **76**, 79-90.

Hamer, K. M., Sewalt, R. G., den Blaauwen, J. L., Hendrix, T., Satijn, D. P. and Otte, A. P. (2002). A panel of monoclonal antibodies against human polycomb group proteins. *Hybrid. Hybridomics* **21**, 245-252.

Hashido, K., Morita, T., Matsushiro, A. and Nozaki, M. (1991). Gene expression of cytokeratin endo A and endo B during embryogenesis and in adult tissues of mouse. *Exp. Cell. Res.* **192**, 203-212.

Healy, A. M., Rayburn, H. B., Rosenberg, R. D. and Weiler, H. (1995). Absence of the blood-clotting regulator thrombomodulin causes embryonic lethality in mice before development of a functional cardiovascular system. *Proc. Natl. Acad. Sci. USA* **92**, 850-854.

Heard, E., Rougeulle, C., Arnaud, D., Avner, P., Allis, C. D. and Spector, D. L. (2001). Methylation of histone H3 at Lys-9 is an early mark on the X chromosome during X inactivation. *Cell* **107**, 727-738.

Hogan, B. L. M. and Newman, R. (1984). A scanning electron microscope

study of the extraembryonic endoderm of the 8th-day mouse embryo. *Differentiation* **26**, 138-143.

Hogan, B. L., Cooper, A. R. and Kurkinen, M. (1980). Incorporation into Reichert's membrane of laminin-like extracellular proteins synthesized by parietal endoderm cells of the mouse embryo. *Dev. Biol.* **80**, 289-300.

Hogan, B. L., Beddington, R., Costantini, F. and Lacy, E. (1994). *Manipulating the Mouse eEbryo: A Laboratory Manual*, 2nd edn. Cold Spring Harbor, NY, Cold Spring Harbor Laboratory Press.

Hogan, B. L. and Tilly, R. (1981). Cell interactions and endoderm differentiation in cultured mouse embryos. *J. Embryol. Exp. Morphol.* **62**, 379-394.

Kanai-Azuma, M., Kanai, Y., Gad, J. M., Tajima, Y., Taya, C., Kurohmaru, M., Sanai, Y., Yonekawa, H., Yazaki, K., Tam, P. P. and Hayashi, Y. (2002). Depletion of definitive gut endoderm in Sox17-null mutant mice. *Development* **129**, 2367-2379.

Kanungo, J., Potapova, I., Malbon, C. C. and Wang, H. (2000). MEKK4 mediates differentiation in response to retinoic acid via activation of c-Jun N-terminal kinase in rat embryonal carcinoma P19 cells. *J. Biol. Chem.* **275**, 24032-24039.

Koutsourakis, M., Langeveld, A., Patient, R., Beddington, R. and Grosveld, F. (1999). The transcription factor GATA6 is essential for early extraembryonic development. *Development* **126**, 723-732.

Lin, T. P. (1969). Microsurgery of inner cell mass of mouse blastocysts. *Nature* **222**, 480-481.

Liu, G., Loraine, A. E., Shigeta, R., Cline, M., Cheng, J., Valmeekam, V., Sun, S., Kulp, D. and Siani-Rose, M. A. (2003). NetAffx: Affymetrix probesets and annotations. *Nucleic Acids Res.* **31**, 82-86.

Mak, W., Baxter, J., Silva, J., Newall, A. E., Otte, A. P. and Brockdorff, N. (2002). Mitotically stable association of polycomb group proteins eed and enx1 with the inactive X chromosome in trophoblast stem cells. *Curr. Biol.* **12**, 1016-1020.

Marotti, K. R., Belin, D. and Strickland, S. (1982). The production of distinct forms of plasminogen activator by mouse embryonic cells. *Dev. Biol.* **90**, 154-159.

Martin, G. R. (1981). Isolation of a pluripotent cell line from early mouse embryos cultured in medium conditioned by teratocarcinoma stem cells. *Proc. Natl. Acad. Sci. USA* **78**, 7634-7638.

Mason, I. J., Taylor, A., Williams, J. G., Sage, H. and Hogan, B. L. (1986). Evidence from molecular cloning that SPARC, a major product of mouse embryo parietal endoderm, is related to an endothelial cell 'culture shock' glycoprotein of Mr 43,000. *EMBO J.* **5**, 1465-1472.

Mercola, M., Wang, C. Y., Kelly, J., Brownlee, C., Jackson-Grusby, L., Stiles, C. and Bowen-Pope, D. (1990). Selective expression of PDGF A and its receptor during early mouse embryogenesis. *Dev. Biol.* **138**, 114-122.

Miquerol, L., Gertsenstein, M., Harpal, K., Rossant, J. and Nagy, A. (1999). Multiple developmental roles of VEGF suggested by a LacZ-tagged allele. *Dev. Biol.* **212**, 307-322.

Mitsui, K., Tokuzawa, Y., Itoh, H., Segawa, K., Murakami, M., Takahashi, K., Maruyama, M., Maeda, M. and Yamanaka, S. (2003). The homeoprotein Nanog is required for maintenance of pluripotency in mouse epiblast and ES cells. *Cell* **113**, 631-642.

Morey, C., Arnaud, D., Avner, P. and Clerc, P. (2001). Tsix-mediated repression of Xist accumulation is not sufficient for normal random X inactivation. *Hum. Mol. Genet.* **10**, 1403-1411.

Morey, C., Navarro, P., Debrand, E., Avner, P., Rougeulle, C. and Clerc, P. (2004). The region 3′ to Xist mediates X chromosome counting and H3 Lys-4 dimethylation within the Xist gene. *EMBO J.* **23**, 594-604.

Morris, S. M., Tallquist, M. D., Rock, C. O. and Cooper, J. A. (2002). Dual roles for the Dab2 adaptor protein in embryonic development and kidney transport. *EMBO J.* **21**, 1555-1564.

Nagy, A., Rossant, J., Nagy, R., Abramow-Newerly, W. and Roder, J. C. (1993). Derivation of completely cell culture-derived mice from early-passage embryonic stem cells. *Proc. Natl. Acad. Sci. USA* **90**, 8424-8428.

Narita, N., Bielinska, M. and Wilson, D. B. (1997). Wild-type endoderm abrogates the ventral developmental defects associated with GATA-4 deficiency in the mouse. *Dev. Biol.* **189**, 270-274.

Notarianni, E. and Flechon, J. (2001). Parietal endoderm cell line from a rat blastocyst. *Placenta* **22**, 111-123.

Okamoto, I., Otte, A. P., Allis, C. D., Reinberg, D. and Heard, E. (2004). Epigenetic dynamics of imprinted X inactivation during early mouse development. *Science* **303**, 644-649.

Oshima, R. G. (1981). Identification and immunoprecipitation of cytoskeletal proteins from murine extra-embryonic endodermal cells. *J. Biol. Chem.* **256**, 8124-8133.

Palmieri, S. L., Peter, W., Hess, H. and Scholer, H. R. (1994). Oct-4 transcription factor is differentially expressed in the mouse embryo during establishment of the first two extraembryonic cell lineages involved in implantation. *Dev. Biol.* **166**, 259-267.

Penny, G. D., Kay, G. F., Sheardown, J. A., Rastan, S. and Brockdorff, N. (1996). Requirement for Xist in X chromosome inactivation. *Nature* **379**, 131-137.

Plath, K., Fang, J., Mlynarczyk-Evans, S. K., Cao, R., Worringer, K. A., Wang, H., de la Cruz, C. C., Otte, A. P., Panning, B. and Zhang, Y. (2003). Role of histone H3 lysine 27 methylation in X inactivation. *Science* **300**, 131-135.

Roebroek, A. J., Umans, L., Pauli, I. G., Robertson, E. J., van Leuven, F., van de Ven, W. J. and Constam, D. B. (1998). Failure of ventral closure and axial rotation in embryos lacking the proprotein convertase Furin. *Development* **125**, 4863-4876.

Rogers, M. B., Hosler, B. A. and Gudas, L. J. (1991). Specific expression of a retinoic acid-regulated, zinc-finger gene, Rex-1, in preimplantation embryos, trophoblast and spermatocytes. *Development* **113**, 815-824.

Rossant, J., Zirngibl, R., Cado, D., Shago, M. and Giguère, V. (1991). Expression of a retinoic acid response element-hsplacZ transgene defines specific domains of transcriptional activity during mouse embryogenesis. *Genes Dev.* **5**, 1333-1344.

Semoff, S., Hogan, B. L. and Hopkins, C. R. (1982). Localization of fibronectin, laminin-entactin, and entactin in Reichert's membrane by immunoelectron microscopy. *EMBO J.* **1**, 1171-1175.

Sewalt, R. G., van der Vlag, J., Gunster, M. J., Hamer, K. M., den Blaauwen, J. L., Satijn, D. P., Hendrix, T., van Driel, R. and Otte, A. P. (1998). Characterization of interactions between the mammalian polycomb-group proteins Enx1/EZH2 and EED suggests the existence of different mammalian polycomb-group protein complexes. *Mol. Cell. Biol.* **18**, 3586-3595.

Silva, J., Mak, W., Zvetkova, I., Appanah, R., Nesterova, T. B., Webster, Z., Peters, A. H., Jenuwein, T., Otte, A. P. and Brockdorff, N. (2003). Establishment of histone h3 methylation on the inactive X chromosome requires transient recruitment of Eed-Enx1 polycomb group complexes. *Dev. Cell* **4**, 481-495.

Smith, A. G., Nichols, J., Robertson, M. and Rathjen, P. D. (1992). Differentiation inhibiting activity (DIA/LIF) and mouse development. *Dev. Biol.* **151**, 339-351.

Solter, D., Damjanov, I. and Skreb, N. (1970). Ultrastructure of mouse egg-cylinder. *Z. Anat. Entwicklungsgesch* **132**, 291-298.

Srinivas, S., Rodriguez, T., Clements, M., Smith, J. C. and Beddington, R. S. (2004). Active cell migration drives the unilateral movements of the anterior visceral endoderm. *Development* **131**, 1157-1164.

Takagi, N. and Sasaki, M. (1975). Preferential inactivation of the paternally derived X chromosome in the extraembryonic membranes of the mouse. *Nature* **256**, 640-642.

Tanaka, S., Kunath, T., Hadjantonakis, A.-K., Nagy, A. and Rossant, J. (1998). Promotion of trophoblast stem cell proliferation by FGF4. *Science* **282**, 2072-2075.

Thomas, P. and Beddington, R. (1996). Anterior primitive endoderm may be responsible for patterning the anterior neural plate in the mouse embryo. *Curr. Biol.* **6**, 1487-1496.

Thomas, P. Q., Brown, A. and Beddington, R. S. (1998). Hex: a homeobox gene revealing peri-implantation asymmetry in the mouse embryo and an early transient marker of endothelial cell precursors. *Development* **125**, 85-94.

Uy, G. D., Downs, K. M. and Gardner, R. L. (2002). Inhibition of trophoblast stem cell potential in chorionic ectoderm coincides with occlusion of the ectoplacental cavity in the mouse. *Development* **129**, 3913-3924.

Veltmaat, J. M., Orelio, C. C., Ward-Van Oostwaard, D., van Rooijen, M. A., Mummery, C. L. and Defize, L. H. (2000). Snail is an immediate early target gene of parathyroid hormone related peptide signaling in parietal endoderm formation. *Int. J. Dev. Biol.* **44**, 297-307.

Verheijen, M. H., Karperien, M., Chung, U., van Wijuen, M., Heystek, H., Hendriks, J. A., Veltmaat, J. M., Lanske, B., Li, E., Lowik, C. W. et al. (1999a). Parathyroid hormone-related peptide (PTHrP) induces parietal endoderm formation exclusively via the type I PTH/PTHrP receptor. *Mech. Dev.* **81**, 151-161.

Verheijen, M. H., Wolthuis, R. M., Bos, J. L. and Defize, L. H. (1999b). The Ras/Erk pathway induces primitive endoderm but prevents parietal endoderm differentiation of F9 embryonal carcinoma cells. *J. Biol. Chem.* **274**, 1487-1494.

Wang, J., Mager, J., Schneider, E. and Magnuson, T. (2002). The mouse

PcG gene eed is required for Hox gene repression and extraembryonic development. *Mamm. Genome* **13**, 493-503.

Wang, S. H., Tsai, M. S., Chiang, M. F. and Li, H. (2003). A novel NK-type homeobox gene, ENK (early embryo specific NK), preferentially expressed in embryonic stem cells. *Gene Expr. Patterns* **3**, 99-103.

Wewer, U. (1982). Characterization of a rat yolk sac carcinoma cell line. *Dev. Biol.* **93**, 416-421.

Yamamoto, M., Saijoh, Y., Perea-Gomez, A., Shawlot, W., Behringer, R. R., Ang, S.-L., Hamada, H. and Meno, C. (2004). Nodal antagonists regulate formation of the anteroposterior axis of the mouse embryo. *Nature* **428**, 387-392.

Yang, D. H., Smith, E. R., Roland, I. H., Sheng, Z., He, J., Martin, W. D., Hamilton, T. C., Lambeth, J. D. and Xu, X. X. (2002). Disabled-2 is essential for endodermal cell positioning and structure formation during mouse embryogenesis. *Dev. Biol.* **251**, 27-44.

Zambrowicz, B. P., Imamoto, A., Fiering, S., Herzenberg, L. A., Kerr, W. G. and Soriano, P. (1997). Disruption of overlapping transcripts in the ROSA beta geo 26 gene trap strain leads to widespread expression of beta-galactosidase in mouse embryos and hematopoietic cells. *Proc. Natl. Acad. Sci. USA* **94**, 3789-3794.

Table S1. RT-PCR primers

Gene name	Forward primer	Reverse primer	Product size (bp)	Annealing temp.	Cycles
AFP	cctgtgaactctggtatcag	gctcacaccaaagcgtcaac	411	52°C	35
Gata4	tcgtaatgccgagggtgagc	tggcctgcgatgtctgagtg	413	60°C	28
Sox7	atgctgggaaagtcatggaag	cgtgttctggtcacgagaga	201	54°C	35
HNF4	tgccctctcacctcagcaatg	cccctcagcacacggttttg	357	55°C	28
Foxa2	ccctacgccaacatgaactcg	gttctgccggtagaaaggga	222	55°C	28
Oct4	ggcgttctctttggaaaggtgttc	ctcgaaccacatccttctct	313	55°C	35
β-actin	ccatcctgcgtctggacctg	gtaacagtccgcctagaagc	620	55°C	23

Primers are in a 5′ to 3′ direction.

Table S2. Gene expression in XEN cells

Affy ID	Unigene	Gene name/symbol	XEN1-3	IM8A1-I	IM8A1-II	ES cells	Ratio
Structural proteins							
103729_at	**Mm.243**	**Laminin, alpha 1**	6066	9260	6375	142	5.5±0.3
92366_at	Mm.256087	Laminin, alpha 2	A	A	A	A	NS
97790_s_at	Mm.42012	Laminin, alpha 3	A	A	A	A	NS
104587_at	Mm.258065	Laminin, alpha 4	A	190	69*	A	NS
99931_at	Mm.4339	Laminin, alpha 5	197*	A	211	377	NS
101948_at	**Mm.172674**	**Laminin, beta 1 subunit 1**	2929	4453	3872	109	3.6±0.3
101359_at	**Mm.289706**	**Laminin, beta 2**	186	183	133	55	1.8±0.5
92759_at	Mm.287014	Laminin, beta 3	A	A	A	A	NS
102404_at	Mm.1249	Laminin, gamma 1	25*	21	23	A	NS
100428_at	Mm.4717	Laminin, gamma 2	A	A	A	131	–1.2±0.2
101130_at	Mm.277792	Procollagen, type I, alpha 2	A	A	A	A	NS
98331_at	Mm.249555	Procollagen, type III, alpha 1	A	A	A	17*	NS
101093_at	**Mm.738**	**Procollagen, type IV, alpha 1**	4911	7712	6377	167	5.2±0.2
101039_at	**Mm.181021**	**Procollagen, type IV, alpha 2**	5308	5659	3491	177	4.6±0.4
100285_at	Mm.8069	Procollagen, type IV, alpha 3	A	A	A	A	NS
101774_at	Mm.57110	Procollagen, type IV, alpha 4	A	A	A	A	NS
93220_at	Mm.286892	Procollagen, type IV, alpha 5	A	A	A	29	NS
92567_at	Mm.10299	Procollagen, type V alpha 2	A	A	A	22	NS
95493_at	Mm.2509	Procollagen, type VI, alpha 1	94	76	A	77	NS
93517_at	Mm.1949	Procollagen, type VI, alpha 2	A	A	A	A	NS
93383_at	Mm.6200	Procollagen, type VII, alpha 1	A	A	A	86	NS
98027_at	Mm.269384	Procollagen, type IX, alpha 2	111	94	119	95	NS
92921_at	Mm.212657	Procollagen, type X, alpha 1	A	A	A	A	NS
100481_at	Mm.209715	Procollagen, type XI, alpha 1	A	A	A	A	NS
102261_f_at	Mm.10805	Procollagen, type XIII, alpha 1	A	A	A	A	NS
102262_r_at	Mm.10805	Procollagen, type XIII, alpha 1	A	A	A	A	NS
101881_g_at	Mm.4352	Procollagen, type XVIII, alpha 1	A	A	A	667	–8.0±0.2
99638_at	Mm.4352	Procollagen, type XVIII, alpha 1	A	A	A	694	–4.9±0.4
99842_at	Mm.6252	Procollagen, type XIX, alpha 1	A	A	A	A	NS
100120_at	**Mm.4691**	**Nidogen 1 (Enactin 1)**	445	207	108	30	2.8±0.9
93563_s_at	**Mm.20348**	**Nidogen 2 (Enactin 2)**	1405	1105	1342	546	1.2±0.2
101399_at	Mm.273662	Perlecan	425	744	505	366	NS
92852_at	Mm.193099	Fibronectin 1	235	336	334	736	NS
101046_at	Mm.268000	Vimentin	33*	A	A	A	NS
101009_at	**Mm.289759**	**Krt2-8 (Endo A)**	1358	1962	2737	443	2.2±0.6
94270_at	**Mm.22479**	**Krt1-18 (Endo B)**	1192	2104	3834	554	1.8±0.9
97160_at	**Mm.291442**	**SPARC**	5924	7284	7376	386	3.9±0.2
99074_at	Mm.27239	Villin	A	A	A	A	NS
100084_at	Mm.277812	Villin2	403	400	553	546	NS
Integrins							
98834_at	Mm.5007	Integrin alpha 2	A	A	A	A	NS
102655_at	Mm.33596	Integrin alpha 4	A	A	A	A	NS
102656_at	Mm.33596	Integrin alpha 4	14	A	6*	A	NS
103039_at	**Mm.16234**	**Integrin alpha 5 (fibronectin receptor)**	111	132	109	A	2.2±0.1
95511_at	Mm.225096	Integrin alpha 6	279	158	161	181	NS

93061_at	Mm.179747	Integrin alpha 7	A	A	A	A	NS
100313_at	Mm.220860	Integrin alpha 8	A	A	A	A	NS
93961_at	Mm.96	Integrin alpha E	A	A	A	A	NS
94764_at	Mm.1618	Integrin alpha L	A	A	A	A	NS
100123_f_at	Mm.263396	Integrin beta 1 (fibronectin receptor)	2786	2777	3328	1609	NS
100124_r_at	**Mm.263396**	**Integrin beta 1 (fibronectin receptor)**	696	706	922	300	1.3±0.3
99904_at	Mm.87150	Integrin beta 3	A	A	A	A	NS
103305_at	Mm.213873	Integrin beta 4	A	A	A	A	NS
100601_at	Mm.6424	Integrin beta 5	A	A	A	A	NS
100906_at	Mm.58	Integrin beta 7	A	A	A	151	NS
Catenins and cadherins							
93364_at	Mm.18962	Catenin, alpha 1	615	766	760	1123	NS
92227_s_at	Mm.34637	Catenin, alpha 2	A	A	A	A	NS
92228_at	Mm.34637	Catenin, alpha 2	165	A	A	A	NS
160430_at	Mm.291928	Catenin, beta	1188	1208	1355	1812	NS
98151_s_at	Mm.35738	Catenin, src	331	337	448	283	NS
104121_at	Mm.21990	Jup, Junction plakoglobin	294	524	548	305	NS
98140_at	Mm.35605	E-cadherin (Cadherin 1)	102	93	124	102	NS
102852_at	Mm.257437	N-cadherin (Cadherin 2)	A	A	A	37	–5.0±0.9
101730_at	**Mm.57048**	**Cadherin 6**	136	120	327	A	3.4±0.9
101701_at	Mm.41976	Cadherin 8	A	A	A	A	NS
94640_at	Mm.8064	Cadherin 9	A	A	A	A	NS
104743_at	Mm.21069	Cadherin 13	A	A	A	A	NS
103213_at	Mm.1976	Cadherin 15	A	A	A	A	NS
93515_at	Mm.19423	Cadherin 16	A	A	A	A	NS
FGF signaling							
100494_at	Mm.241282	FGF1	A	A	A	A	NS
93216_at	Mm.57094	FGF2	A	A	A	A	NS
92957_at	Mm.4947	FGF3	A	102	A	A	NS
98826_at	Mm.4956	FGF4	172*	A	A	1056	–2.5±0.2
98845_at	Mm.5055	FGF5	A	A	A	A	NS
97121_at	Mm.3403	FGF6	A	A	A	A	NS
99435_at	Mm.57177	FGF7	15	A	A	A	NS
97742_s_at	Mm.4012	FGF8	A	A	A	A	NS
100346_at	Mm.8846	FGF9	A	A	A	A	NS
95976_at	Mm.25003	FGF10	A	A	A	A	NS
102574_at	Mm.269011	FGF11	A	A	A	A	NS
93654_at	Mm.7996	FGF12	A	A	A	A	NS
99893_at	Mm.7995	FGF13	A	A	A	A	NS
99424_at	Mm.32472	FGF14	A	A	A	A	NS
97721_at	Mm.3904	FGF15	A	A	A	38*	NS
98730_at	Mm.12814	FGF17	A	A	A	123	–4.6±0.7
95316_at	Mm.246671	FGF18	A	A	A	A	NS
97509_f_at	Mm.265716	FGFR1	A	A	A	206	–3.5±0.9
93090_at	Mm.16340	FGFR2	A	A	A	206	–1.1±0.3
160919_r_at	Mm.6904	FGFR3	A	8*	21	12	NS
92937_at	Mm.276715	FGFR4	A	A	A	A	NS

98278_at	Mm.42038	Sprouty4	147	103	69	64	NS
161070_at	Mm.114382	Spred2	135	143	137	215	NS
PDGF, VEGF and EGF signaling							
94932_at	Mm.2675	PDGF-A	181	137	183	451	–1.8±0.3
99890_at	Mm.144089	PDGF-B	A	A	A	A	NS
95079_at	**Mm.221403**	**PDGFRa**	1057	1487	1056	A	7.5±0.3
160867_at	Mm.4146	PDGFRβ	A	A	A	A	NS
103520_at	**Mm.31540**	**VEGF-A**	112	263	158	54	2.1±0.4
103001_at	Mm.15607	VEGF-B	472	344	344	268	NS
94712_at	Mm.1402	VEGF-C	A	65	A	A	NS
99936_at	Mm.4345	Tie1	A	A	A	A	NS
98452_at	**Mm.241483**	**Flt-1**	60	65	174	21*	1.4±0.9
104265_at	Mm.285	Flk-1	A	A	A	A	NS
102774_at	Mm.254772	EGF	A	A	A	A	NS
101840_at	Mm.8534	EGFR	A	A	A	A	NS
101841_at	Mm.8534	EGFR	A	A	A	A	NS
101842_g_at	Mm.8534	EGFR	A	A	A	A	NS
Ephrins and Eph receptors							
103007_at	Mm.15675	Ephrin A1	A	A	A	A	NS
100289_at	Mm.8547	Ephrin A3	463	407	485	287	NS
103041_at	Mm.16332	Ephrin A4	71	83	99	A	NS
99887_at	Mm.7978	Ephrin A5	A	A	A	A	NS
98407_at	Mm.3374	Ephrin B1	A	A	A	A	NS
160857_at	**Mm.209813**	**Ephrin B2**	257	495	196	93	1.5±0.7
94160_at	Mm.249637	Ephrin B3	A	89	A	A	NS
103980_at	Mm.2581	Eph receptor A2	A	A	A	236	–1.2±0.5
95298_at	Mm.1977	Eph receptor A3	A	A	A	A	NS
104673_at	Mm.3249	Eph receptor A4	28	63	65	39	NS
92905_at	Mm.260354	Eph receptor A7	A	A	A	A	NS
92906_at	Mm.260354	Eph receptor A7	A	A	A	A	NS
102682_at	Mm.1390	Eph receptor A8	53	56*	A	43*	NS
98771_at	Mm.250981	Eph receptor B2	73	57	44	46	NS
93469_at	**Mm.6972**	**Eph receptor B3**	910	1053	399	88*	2.3±0.8
98446_s_at	Mm.34533	Eph receptor B4	1320	880	992	2393	–1.3±0.3
Ras/MAPK signaling							
101034_at	Mm.6900	Grb2	124	140	154	126	NS
160911_at	Mm.6357	Sos1	80	77	92	134	NS
92302_at	**Mm.3770**	**Sos2**	116	76	82	28	1.9±0.3
160925_at	Mm.256975	N-Ras	223	374	258	218	NS
97991_at	Mm.207540	K-Ras2	243	221	313	327	NS
94913_at	Mm.290530	RasGAP	354	350	432	478	NS
94264_at	Mm.289737	Raf1	297	388	242	248	NS
103022_at	Mm.15918	Map3k1, MEKK1	A	A	A	A	NS
101175_at	Mm.211762	Map3k2, MEKK2	A	A	A	A	NS
94946_at	**Mm.27041**	**Map3k3, MEKK3**	133	112	120	47	1.1±0.1
94947_g_at	**Mm.27041**	**Map3k3, MEKK3**	195	159	155	53	1.1±0.2

104272_s_at	Mm.28587	Map3k4, MEKK4	218	125	137	170	NS
92585_at	Mm.248907	Map2k1, MAPKK1	265	351	377	583	NS
99960_at	Mm.27491	Map2k4, MAPKK4	149	159	159	119	NS
103592_at	Mm.192651	Map2k5, MAPKK5	194	167	162	113	NS
99036_s_at	Mm.3906	Map2k7, MAPKK7	32	A	A	A	NS
99037_at	Mm.3906	Map2k7, MAPKK7	A	A	A	A	NS
93253_at	Mm.196581	MAPK1 (ERK2)	99	138	171	134	NS
93254_at	Mm.196581	MAPK1 (ERK2)	719	1098	1169	996	NS
101834_at	Mm.8385	MAPK3 (ERK1)	81	53	88	132	NS
103416_at	Mm.18856	MAPK6 (ERK3)	609	500	744	1038	NS
99000_at	Mm.38172	MAPK7 (ERK5)	90*	115	A	130	NS
104047_at	Mm.21495	MAPK8 (JNK)	136	185	158	170	NS
101362_at	Mm.68933	MAPK9 (JNK2)	40	54	47	29	NS
100470_at	Mm.299388	MAPK10 (JNK3)	A	A	A	A	NS
Wnt signaling							
94134_at	Mm.1123	Wnt1	A	A	A	A	NS
94126_at	Mm.10740	Wnt2b	A	A	A	A	NS
99325_at	Mm.5188	Wnt3	A	A	A	52	NS
102667_at	Mm.1367	Wnt3a	A	A	A	A	NS
103238_at	Mm.20355	Wnt4	A	A	A	A	NS
99390_at	Mm.287544	Wnt5a	A	A	A	A	NS
103513_at	Mm.22622	Wnt5b	A	A	A	A	NS
103735_at	Mm.268282	Wnt6	A	A	A	A	NS
101316_at	Mm.56964	Wnt7a	A	A	A	A	NS
92404_at	Mm.4092	Wnt7b	63*	A	A	A	NS
99361_at	Mm.558	Wnt8a	A	A	A	A	NS
98862_at	Mm.278101	Wnt10a	38	41	30	29	NS
92750_s_at	Mm.4709	Wnt10b	A	A	A	A	NS
92751_i_at	Mm.4709	Wnt10b	A	8	10	6	NS
92752_r_at	Mm.4709	Wnt10b	A	A	A	A	NS
103490_at	**Mm.22182**	**Wnt11**	153	103	65	A	5.3±0.6
104672_at	**Mm.136022**	**Frzb, Frizzled-related protein**	940	180	144	A	6.5±1.4
161040_at	Mm.246003	Frizzled 1	A	A	A	A	NS
98348_at	Mm.243722	Frizzled 3	A	A	A	A	NS
95771_i_at	Mm.86755	Frizzled 4	A	A	A	A	NS
95772_r_at	Mm.86755	Frizzled 4	A	A	A	A	NS
101142_at	Mm.4769	Frizzled 6	A	43	42	A	NS
101143_at	Mm.297906	Frizzled 7	53*	83	71	A	NS
99415_at	Mm.184289	Frizzled 8	A	53*	51	46	NS
99844_at	Mm.6256	Frizzled 9	A	A	A	A	NS
97997_at	Mm.281691	Sfrp1, Secreted frizzled-related protein 1	A	A	A	54	–3.4±1.0
93503_at	Mm.19155	Sfrp2, Secreted frizzled-related protein 2	A	A	A	109	NS
92469_at	Mm.42095	Sfrp4, Secreted frizzled-related protein 4	A	A	A	A	NS
99881_at	Mm.214717	Dickkopf1	A	88	44	A	NS
161117_at	Mm.103593	Dickkopf2	A	A	A	A	NS
93188_at	Mm.55143	Dickkopf3	A	A	A	A	NS

TGFβ signaling							
101918_at	Mm.9154	TGFβ1	A	A	A	A	NS
93300_at	Mm.18213	TGFβ2	A	A	A	A	NS
102751_at	Mm.3992	TGFβ3	A	A	54*	A	NS
102559_at	Mm.235230	BMP2	A	63	A	A	NS
93455_s_at	Mm.6813	BMP4	85	59	68	238	NS
93456_r_at	Mm.6813	BMP4	16	A	4*	168	NS
99393_at	Mm.118034	BMP5	A	A	A	A	NS
92372_at	Mm.254978	BMP6	50	40	62	A	NS
93243_at	Mm.595	BMP7	A	A	A	A	NS
92982_at	Mm.5044	BMP8a	A	A	A	A	NS
101657_at	Mm.30413	BMP8b	A	A	A	A	NS
99801_at	Mm.57195	Nodal	A	A	A	245	–3.7±0.2
100515_at	**Mm.243921**	**Furin**	450	327	455	199	1.0±0.3
97727_at	**Mm.39094**	**Noggin**	263	351	121	A	3.2±0.8
103249_at	Mm.20457	Chordin	A	A	A	A	NS
98817_at	**Mm.4913**	**Follistatin**	1869	3475	2990	A	5.8±0.5
93452_at	Mm.6780	Cerberus 1	A	A	A	A	NS
94702_at	Mm.172346	Tgfbr2, type II	A	A	A	A	NS
100450_r_at	Mm.279542	Acvrl1, (ALK-1)	A	A	A	A	NS
93460_at	**Mm.689**	**Acvr1, Activin A receptor, type 1**	93	65	64	A	4.3±0.3
101177_at	Mm.5070	Acvr1b, Activin A receptor, type 1B	A	A	A	A	NS
98841_at	Mm.247684	Acvr2, Activin receptor IIA	40	33	26	21	NS
93903_at	Mm.8940	Acvr2b, Activin receptor IIB	403	201	181	595	–1.5±0.5
92767_at	**Mm.237825**	**Bmpr1a, BMP receptor, type 1A**	134	75	117	59	1.1±0.5
99865_at	Mm.7106	Bmpr2, BMP receptor, type II	59*	43	55	A	NS
100635_at	Mm.6698	Sara1	1256	1027	802	599	NS
102983_at	Mm.223717	SMAD1	94	169	191	99	NS
102984_g_at	Mm.223717	SMAD1	152	308	266	185	NS
104536_at	Mm.152699	SMAD2	208	521	515	151	NS
93613_at	Mm.7320	SMAD3	A	A	A	A	NS
160440_at	Mm.100399	SMAD4	460	666	668	396	NS
102865_at	Mm.272920	SMAD5	A	23	20*	25*	NS
104220_at	Mm.27935	SMAD6	A	A	109	85	NS
92216_at	Mm.34407	SMAD7	118	190	154	332	–1.0±0.3
Hedgehog signaling							
101831_at	Mm.57202	Sonic hedgehog	A	A	A	A	NS
103949_at	Mm.2543	Indian hedgehog	182	63	156	29*	NS
99861_at	Mm.272135	Desert hedgehog	A	A	A	A	NS
104031_at	Mm.138472	Ptc1	56	A	A	58	NS
96557_at	Mm.287037	Ptc2	A	A	A	99	–2.6±0.8
96812_at	**Mm.29279**	**Smoothened**	126	128	100	60	1.0±0.2
94097_at	Mm.298131	Gli1	A	A	A	108	–2.3±1.0
100395_at	Mm.273292	Gli2	A	A	A	130	–2.7±0.5
101182_at	Mm.5098	Gli3	A	A	A	A	NS

gp130/JAK/STAT signaling							
94345_at	Mm.4364	IL-6 signal transducer (gp130)	189	117	92	160	NS
98349_at	Mm.4364	IL-6 signal transducer (gp130)	92	50	45	46	NS
104657_at	**Mm.149720**	**LIF receptor**	68	68	85	A	2.6±0.1
104658_at	**Mm.149720**	**LIF receptor**	168	168	269	A	2.4±0.3
104659_g_at	**Mm.149720**	**LIF receptor**	162	162	244	A	2.7±0.5
97006_s_at	Mm.149720	LIF receptor	36	69	50	A	NS
102658_at	Mm.1349	Interleukin 1 receptor, type II	A	27	35	A	NS
100764_at	Mm.35287	Interleukin 2 receptor, beta	A	A	A	A	NS
101917_at	Mm.915	Interleukin 2 receptor, alpha	A	A	A	A	NS
102021_at	Mm.233802	Interleukin 4 receptor, alpha	A	A	A	A	NS
104268_at	Mm.2856	Interleukin 6 receptor, alpha	A	A	A	A	NS
162408_f_at	Mm.731	Interleukin 12 receptor, beta 1	A	A	A	A	NS
98240_at	Mm.731	Interleukin 12 receptor, beta 1	A	A	A	A	NS
99323_at	Mm.188337	Interleukin 12 receptor, beta 2	A	A	A	A	NS
103723_at	Mm.24208	Interleukin 13 receptor, alpha 1	A	A	A	A	NS
95344_at	Mm.20855	Interleukin 13 receptor, alpha 2	A	A	A	A	NS
101144_at	Mm.253664	Interleukin 18 receptor 1	A	A	A	A	NS
101651_at	Mm.270210	Ciliary neurotrophic factor receptor	A	A	A	A	NS
102255_at	Mm.10760	Oncostatin M receptor	17*	23	26	A	NS
93198_at	Mm.271701	Colony stimulating factor 3 receptor	A	A	A	A	NS
98911_at	Mm.289657	JAK1	156	201	210	203	NS
101457_at	**Mm.275839**	**JAK2**	79	86	114	A	1.3±0.4
99509_s_at	Mm.247327	JAK3	A	A	A	158	NS
97573_at	Mm.239803	Tyk2	A	A	A	A	NS
101465_at	Mm.277406	STAT1	13	29	21	18	NS
99099_at	Mm.249934	STAT3	410	558	441	301	NS
99100_at	Mm.249934	STAT3	214	389	294	167	NS
102994_at	Mm.1550	STAT4	A	A	A	53	NS
100422_i_at	Mm.277403	STAT5a	A	188	233	160*	NS
100423_f_at	Mm.277403	STAT5a	A	A	A	A	NS
92199_at	Mm.34064	STAT5b	A	A	A	A	NS
94331_at	Mm.121721	STAT6	A	A	A	179	–4.1±0.7
PKC family							
102299_at	Mm.234258	PKC, alpha	A	43	A	A	NS
99510_at	Mm.207496	PKC, beta	A	A	A	105	NS
99511_at	Mm.207496	PKC, beta	A	A	A	A	NS
93648_at	Mm.7980	PKC, gamma	A	A	A	A	NS
160698_s_at	Mm.2314	PKC, delta	427	358	364	327	NS
94161_at	**Mm.240216**	**PKC, epsilon**	125	105	63	A	1.9±0.5
101148_at	Mm.291554	PKC, lambda	72	34	65	67	NS
99581_at	Mm.425	PKC inhibitor	3181	3506	2427	1957	NS
Rab family							
92882_at	Mm.271944	Rab1	264	369	465	305	NS
94031_at	Mm.240224	Rab2	308	484	479	258	NS
160524_at	Mm.5083	Rab3a	A	A	A	A	NS

101921_at	**Mm.9221**	**Rab4a**	320	289	534	194	1.0±0.5
98731_at	Mm.12815	Rab5b	91	58*	77	58*	NS
99587_at	Mm.4268	Rab7	265	438	674	281	NS
101933_at	Mm.74596	Rab10	90	146	131	84	NS
92854_at	Mm.1387	Rab11a	900	699	1435	565	NS
98150_at	Mm.35727	Rab11b	232	232	272	190	NS
97301_at	Mm.29302	Rab14	808	797	704	745	NS
92329_at	Mm.279780	Rab17	A	A	A	A	NS
94319_at	Mm.132802	Rab18	907	954	876	1272	NS
93718_at	Mm.86744	Rab23	53	49	43	54	NS
93347_at	Mm.271157	Rab24	957	502	524	380	NS
103062_at	Mm.1664	Rab33b	107	86	98	A	NS
94269_at	Mm.273561	Rabac1, Rab acceptor 1	711	480	534	815	NS
Various transcription factors							
102654_at	Mm.1344	Gata1	A	A	A	A	NS
102789_at	Mm.272747	Gata2	A	A	A	A	NS
100924_at	Mm.606	Gata3	A	30*	23	19*	NS
102713_at	**Mm.161558**	**Gata4**	1091	1196	899	A	4.4±0.3
96500_at	Mm.2527	Gata5	A	A	A	A	NS
104698_at	**Mm.24912**	**Gata6**	2468	1973	1086	A	5.8±0.7
97974_at	**Mm.3105**	**FOG1, Friend of GATA-1**	300	276	238	A	1.3±0.2
92342_at	Mm.39088	Sox1	A	A	A	A	NS
100009_r_at	Mm.51994	Sox2	A	A	A	3391	–9.5±1.0
92264_at	Mm.35784	Sox3	A	A	A	A	NS
160109_at	Mm.240627	Sox4	A	A	150	110	NS
102954_at	Mm.1752	Sox5	A	A	A	A	NS
92726_at	Mm.4656	Sox6	A	A	A	A	NS
92487_at	**Mm.42162**	**Sox7**	981	1339	225	A	4.7±1.3
102856_at	Mm.276739	Sox10	58	71	A	65	NS
101631_at	Mm.41702	Sox11	A	A	A	248	–2.4±0.1
93698_at	Mm.8575	Sox13	A	367	340	264	NS
92997_g_at	**Mm.279103**	**Sox17**	1024	1436	1285	A	8.7±0.3
92996_at	**Mm.279103**	**Sox17**	1293	1895	1712	A	7.1±0.2
104408_s_at	Mm.264904	Sox18	A	A	A	A	NS
93945_at	Mm.9213	ERa	A	A	A	A	NS
96514_at	Mm.2561	ERβ	A	A	A	A	NS
103964_at	Mm.260481	ERRa	244	246	206	124	NS
100301_at	Mm.235550	ERRβ	A	A	A	A	NS
92901_at	Mm.103336	RARa	A	61	44*	A	NS
102419_at	Mm.1273	RARγ	A	A	A	A	NS
92234_at	Mm.3470	RXRa	A	A	A	A	NS
92235_g_at	Mm.3470	RXRa	A	A	A	111	NS
92237_at	Mm.3475	RXRγ	A	A	A	A	NS
101396_at	**Mm.7226**	**Tcf2 (HNF1β, vHNF1)**	111	189	138	A	6.5±0.2
92697_at	Mm.4578	Foxa1 (HNF3a)	A	A	A	A	NS
93950_at	**Mm.938**	**Foxa2 (HNF3β)**	552	512	520	A	5.7±0.1
98324_at	Mm.42260	Foxa3, (HNF3γ)	A	48*	82	A	NS
92713_at	Mm.202383	HNF4	A	A	A	A	NS

101704_at	Mm.41985	HNF4γ	A	A	A	A	NS
98408_at	Mm.33896	Hex	75	51	71	59	NS
98804_at	Mm.4802	Hesx1	A	A	A	A	NS
100717_at	Mm.2093	Snail	590	660	239	154	NS
99552_at	Mm.4272	Snail2 (Slug)	A	A	A	85*	NS
103477_at	Mm.144448	Cdx1	A	A	A	A	NS
103239_at	Mm.20358	Cdx2	A	A	A	A	NS
98347_at	Mm.4353	Cdx4	A	A	A	A	NS
160705_at	**Mm.2390**	**Cited1 (Msg1)**	1208	1032	1651	106*	3.5±0.4
94187_at	Mm.129	Goosecoid	A	A	A	A	NS
102972_s_at	Mm.289682	Disabled1	A	35	A	A	NS
98044_at	**Mm.240830**	**Disabled2**	206	277	624	A	2.6±0.7
98045_s_at	**Mm.240830**	**Disabled2**	1925	2334	4937	42*	6.0±0.6
103075_at	Mm.17031	Pou5f1 (Oct4)	A	A	A	3191	–10.5±0.6
161072_at	Mm.6047	Nanog	A	A	A	3275	–7.6±0.3
98414_at	Mm.285848	Zfp42 (Rex1)	A	A	A	1232	–7.3±1.3
93880_at	Mm.200692	Eomesodermin	A	A	A	A	NS
103532_at	Mm.200692	Eomesodermin	A	A	A	17*	NS
93941_at	Mm.913	Brachyury	A	A	A	142	–4.8±1.1
Other genes							
103957_at	Mm.28683	Transferrin receptor	35	30	59	104	–1.3±0.4
103958_g_at	Mm.28683	Transferrin receptor	347	540	710	520	NS
160832_at	Mm.3213	LDLR, Low density lipoprotein receptor	767	230	682	400	NS
96047_at	**Mm.2605**	**RBP4, Retinol binding protein 4**	130	171	2671	A	6.2±2.4
98320_at	**Mm.42230**	**Cyp26a1 (P450RAI)**	354	1721	1010	17	5.7±1.0
102258_at	**Mm.10801**	**Stra6**	465	296	85	A	5.1±1.3
102927_s_at	Mm.209071	Huntingtin	234	199	154	230	NS
92547_at	Mm.263318	Huntingtin interacting protein-2	126	100	110	154	NS
92548_g_at	Mm.263318	Huntingtin interacting protein-2	168	101	142	127	NS
103342_at	Mm.18203	Eed	227	188	209	768	–1.8±0.1
99917_at	Mm.246688	Ezh2 (Enx1)	513	590	433	860	NS
104601_at	**Mm.24096**	**Thrombomodulin**	219	393	199	A	4.7±0.6
97772_at	Mm.4183	uPA, urokinase-type plasminogen activator	A	A	A	A	NS
93981_at	**Mm.154660**	**tPA, tissue-type plasminogen activator**	1641	1893	1191	A	5.1±0.6
98482_at	**Mm.248293**	**PTHR1**	2276	2128	1384	A	5.3±0.5
101493_at	Mm.80	AFP, a-fetoprotein	A	A	A	A	NS
101494_at	Mm.80	AFP, a-fetoprotein	A	A	A	A	NS
97940_at	Mm.30271	Placental lactogen 1	A	A	A	A	NS
93883_at	Mm.88796	Proliferin	A	A	A	A	NS

Expression analysis of XEN cells by Affymetrix profiling (from the mouse U74Av2 Affymetrix array). The data from genes of interest are shown. The Affy Clone ID, Unigene designation and gene name or symbol are listed. The three XEN samples (XEN1-3, IM8A1-I and IM8A1-II) are described in the text. If a gene is expressed, its expression level is indicated by a numerical value. An asterisk (*) denotes an expression value that is marginally significant ($0.04<P<0.06$). If a gene is not expressed, it is indicated by 'A' (absent). The average expression ratio (Ratio) between one ES cell sample and the three XEN cell samples is shown with a standard deviation. Positive values indicate the gene is more highly expressed in XEN cells, while negative values indicate higher expression in ES cells. NS indicates no significant difference. Genes more highly expressed in XEN cells are in bold.

Table S3. Top 40 XEN cell-enriched genes in comparison to ES cells

Affy ID	Unigene	Gene name/symbol	Ave. ratio	s.d.
102410_at	Mm.12559	Hs3st1, Heparin sulfate-3-O-sulfotransferase 1	9.7	0.4
102384_at	Mm.268103	RIKEN cDNA 2610209L14	8.9	0.3
92997_g_at	Mm.279103	**Sox17**	8.7	0.3
94085_at	Mm.22194	Prg, Proteoglycan, secretory granule	8.0	0.6
93514_at	Mm.7353	Myl3, Myosin, light polypeptide 3, alkali	7.7	0.8
95079_at	Mm.221403	**PDGFRa**	7.5	0.3
92996_at	Mm.279103	**Sox17**	7.1	0.2
92558_at	Mm.76649	VCAM1	7.0	1.3
94834_at	Mm.2277	Cathepsin H	6.8	1.2
98384_at	Mm.4497	Protein Tyrosine Kinase 6	6.6	0.8
101396_at	Mm.7226	**Tcf2 (HNF1β, vHNF1)**	6.5	0.2
104672_at	Mm.136022	Frzb, Frizzled-related protein	6.5	1.4
160613_at	Mm.15801	Lipocalin 7	6.4	0.3
95000_g_at	Mm.264540	Cubilin	6.3	0.2
92665_f_at	Mm.178800	RIKEN cDNA 3830403N18	6.3	1.7
92374_at	Mm.269621	Myosin binding protein H	6.3	0.5
103059_at	Mm.263847	Fxyd3, FYXD domain-containing ion transport regulator 3	6.3	0.6
96047_at	Mm.2605	Rbp4, Retinol binding protein 4, plasma	6.2	2.4
96588_at	Mm.30424	Ptger3, Prostaglandin E receptor 3 (subtype EP3)	6.1	2.2
98045_s_at	Mm.240830	**Disabled2**	6.0	0.6
93328_at	Mm.18603	Histidine decarboxylase	5.9	0.9
104698_at	Mm.264912	**Gata6**	5.8	0.7
98817_at	Mm.4913	**Follistatin**	5.8	0.5
96122_at	Mm.28108	RIKEN cDNA 2310016A09	5.8	1.0
162023_f_at	Mm.24096	**Thrombomodulin**	5.7	0.2
92306_at	Mm.3782	Ott, Ovary testis transcribed	5.7	1.0
102258_at	Mm.10801	**Stra6**	5.7	1.2
93950_at	Mm.938	**Foxa2 (HNF3β)**	5.7	0.1
103729_at	Mm.243	Laminin, alpha 1	5.5	0.3
103830_at	Mm.2093	**Snail**	5.5	0.7
103227_at	Mm.281844	AI788959	5.4	1.1
98482_at	Mm.248293	**PTHR1**	5.3	0.6
103490_at	Mm.22182	Wnt11	5.3	0.5
102048_at	Mm.10279	Ankrd1, Ankyrin repeat domain 1	5.3	0.8
101093_at	Mm.738	Procollagen, type IV, alpha 1	5.2	0.5
102373_at	Mm.1193	Enpep, Glutamyl aminopeptidase	5.2	0.2
97689_at	Mm.3742	Coagulation factor III	5.2	0.2
98320_at	Mm.42230	**Cyp26a1 (P450RAI)**	5.1	1.2
93981_at	Mm.154660	**tPA, tissue-type plasminogen activator**	5.1	0.6
97504_at	Mm.3141	Cyclin D2	5.1	0.5

Affymetrix expression data set for three XEN cell samples (XEN1-3, IM8A1-I, IM8A1-II) compared to an ES cell data set using Affymetrix MAS 5.0 software. The three log ratio values (XEN/ES) for each gene were averaged (Ave. ratio) and the standard deviation (s.d.) calculated. The top 40 XEN cell-enriched genes are listed and genes in bold are known to be expressed in extra-embryonic endoderm (see Table 1). The Change *P*-values for all 40 genes were $P<0.002$.

Table S4. Top 15 ES cell-enriched genes in comparison to XEN cells

Affy ID	Unigene	Gene name/symbol	Ave. ratio	s.d.
160370_at	Mm.139314	**Dppa5, Developmental pluripotency associated 5 (Esg1)**	–10.7	1.0
103075_at	Mm.17031	**Pou5f1 (Oct4)**	–10.5	0.6
100009_r_at	Mm.51994	**Sox2**	–9.5	1.0
94334_f_at	Mm.276251	Ina, Internexin neuronal intermediate filament protein, α	–8.4	1.7
97834_g_at	Mm.273874	Pfkp, Phosphofructokinase, platelet	–8.3	1.3
97519_at	Mm.288474	**Osteopontin (Spp1)**	–8.0	0.9
101881_g_at	Mm.4352	Procollagen, type XVIII, alpha 1	–8.0	0.2
161072_at	Mm.6047	**Nanog**	–7.6	0.3
98414_at	Mm.285848	**Zfp42 (Rex1)**	–7.3	1.3
94335_r_at	Mm.276251	Ina, Internexin neuronal intermediate filament protein, α	–6.6	1.2
93141_at	Mm.5180	Nr0b1 (Dax1)	–6.5	0.9
97833_at	Mm.273874	Pfkp, Phosphofructokinase, platelet	–6.4	1.4
102220_at	Mm.10205	**Utf1, Undifferentiated embryonic cell TF1**	–6.3	0.5
92258_at	Mm.35597	**Dppa4, Developmental pluripotency associated 4**	–6.3	1.3
98330_at	Mm.255890	Zic3	–5.9	0.9

The top 15 ES cell-enriched genes with respect to XEN cells from the analysis described in Table S3. The genes in bold are known ES cell-associated genes.

References

Dppa5 (Esg1): Bierbaum, P., MacLean-Hunter, S., Ehlert, F., Moroy, T. and Muller, R. (1994) *Cell Growth Differ.* **5**, 37-46.
Pou5f1 (Oct4): Palmieri, S. L., Peter, W., Hess, H. and Schöler, H. R. (1994). *Dev. Biol.* **166**, 259-267.
Sox2: Avilion, A. A., Nicolis, S. K., Pevny, L. H., Perez, L., Vivian, N. and Lovell-Badge, R. (2003). *Genes Dev.* **17**, 126-140.
Osteopontin (Spp1): Botquin, V., Hess, H., Fuhrmann, G., Anastassiadis, C., Gross, M. K., Vriend, G. and Schöler, H. R. (1998). *Genes Dev.* **12**, 2073-2090.
Nanog: Wang, S. H., Tsai, M. S., Chiang, M. F. and Li, H. (2003). *Gene Expr. Patterns* **3**, 99-103.
Zfp42 (Rex1): Rogers, M. B., Hosler, B. A. and Gudas, L. J. (1991). *Development* **113**, 815-824.
Utf1: Okuda, A., Fukushima, A., Nishimoto, M., Orimo, A., Yamagishi, T., Nabeshima, Y., Kuro-o, M., Nabeshima, Y., Boon, K., Keaveney, M. et al. (1998). *EMBO J.* **17**, 2019-2032.
Dppa4: Bortvin, A., Eggan, K., Skaletsky, H., Akutsu, H., Berry, D. L., Yanagimachi, R., Page, D. C. and Jaenisch, R. (2003). *Development* **130**, 1673-1680.